ABSTRACT

WEBB, MATHEW DOUGLAS. Carbon, Chlorine, and Oxygen Isotopes as Tracers of Interbasin Groundwater Flow at La Selva Biological Station, Costa Rica. (Under the direction of Prof. David Genereux.)

Groundwater and surface water samples were taken at 14 locations at a lowland rainforest site (La Selva Biological Station) in Costa Rica for the analysis of DIC, DOC, ^{14}C, ^{13}C, ^{36}Cl, ^{18}O, and other geochemical parameters. The data are consistent with the mixing of two endmember groundwaters. One is a local water having low Cl concentrations (<0.07 mM), low DIC (<3.0 mM), high ^{14}C (>100 pmc), $\delta^{13}C$ between -22‰ and -26‰, and highly variable $^{36}Cl/Cl$ ratios. This chemistry is consistent with locally recharged shallow groundwaters having short residence times in which the DIC originates from plant root respiration and atmospheric deposition is the only source of Cl. The other endmember is bedrock groundwater, representing interbasin groundwater flow (IGF) into La Selva and having relatively high Cl concentration (>0.9 mM), high DIC (about 14 mM), low ^{14}C (<8 pmc), high $\delta^{13}C$ (-3‰ to -5‰), and a low and more consistent $^{36}Cl/Cl$ ratio. This chemistry is consistent with the expectations for bedrock groundwater recharged on the flanks of Volcan Barva to the north of La Selva, with a majority of the DIC and Cl derived from magmatic degassing and dissolution of the volcanic rocks that make up the aquifer. A ^{14}C age of 750 – 4650 years before present was estimated for the bedrock groundwater endmember using NETPATH geochemical mass-balance modeling software, suggesting an average linear velocity of 3-20 m/yr for this groundwater; the actual age is probably closer to the upper limit, and velocity closer to the lower limit. The results of this study are consistent with prior work using major ion, ^{18}O, and physical hydrologic data, suggesting that the conclusions about IGF and

groundwater mixing at this site are correct. Also, new DIC data for bedrock groundwater and previous hydrologic data on bedrock groundwater inputs to the Arboleda watershed at La Selva suggest that IGF of bedrock groundwater is responsible for a large inorganic carbon flux into lowland watersheds (about 740 grams of carbon per m^2 of watershed each year for the Arboleda).

CARBON, CHLORIDE, AND OXYGEN ISOTOPES AS TRACERS OF INTERBASIN GROUNDWATER FLOW AT LA SELVA BIOLOGICAL STATION, COSTA RICA

by
Mathew Webb

A thesis submitted to the graduate faculty of
North Carolina State University
in partial fulfillment of the
requirements for the degree of
Master of Science

MARINE, EARTH, AND ATMOSPHERIC SCIENCES

Raleigh, North Carolina

2007

APPROVED BY:

Professor Neal Blair	**Professor John Fountain**

Professor David Genereux
Chair of Advisory Committee

BIOGRAPHY

Mathew Webb was born in Wooster, Ohio and graduated from Wooster High School in 1998. He obtained a B.S. in Earth Science with specialization in geology and geohydrology from Montana State University in 2003. In May 2007 he obtained an M.S. in Earth Science with a specialization in hydrogeology from North Carolina State University.

ACKNOWLEDGEMENTS

I would like to thank my advisor Dr. David Genereux for his guidance in conducting this research. I would also like to thank the other members of my committee, Dr Neal Blair and Dr. John Fountain, for their insight and advice. In that regard I must also thank Dr. Neil Plummer (USGS in Reston, VA) and Casey Kennedy (NCSU-MEAS) for their insight and assistance in the modeling effort. Thanks also goes to the National Science Foundation for its financial support.

TABLE OF CONTENTS

LIST OF TABLES

LIST OF FIGURES

Chapter 1. Introduction

Interbasin groundwater flow (groundwater flow beneath topographic divides) is often considered a complicating problem in watershed hydrologic studies. In fact, most work with watershed hydrology and geochemistry attempts to avoid interbasin groundwater flow (IGF) by selecting sites that are believed to be "tight" (having no IGF), or nearly so (Bruijnzeel 1990). However, IGF is an expected and common feature of groundwater flow systems. Toth's (1962, 1963) classic work demonstrated the likelihood of IGF through regional-scale groundwater systems beneath smaller, local systems. Toth (1963) showed that IGF is possible even in homogenous, isotropic materials, given the right combination of topography and length/depth ratio of the groundwater system. In more realistic geologic settings with heterogeneity and anisotropy, IGF commonly follows structural and lithostratigraphic controls (Thyne et al. 1999; Parker et al. 1988; Eakin 1966).

The most obvious effect of IGF is to diminish surface water discharge from watersheds that lie in the recharge area of regional aquifers (in which IGF originates), and enhance discharge in watersheds where the regional aquifer discharges (receiving IGF). Noting the much shorter subsurface residence times in small local groundwater systems, Toth (1963) predicted that there would also be large spatial heterogeneities in groundwater chemistry in watersheds with IGF discharge. Watersheds receiving IGF are expected to have complex discharge zones resulting from the mixing of two groundwaters having very different ages and chemistry where old high-solute water from a deeper regional groundwater system mixes with much younger lower-solute groundwater from a smaller, shallower, locally recharged system.

The type of chemical heterogeneity that Toth (1963) predicted has been detected at the Costa Rican lowland rainforest site (La Selva Biological Station) that will be studied here. Major ion concentrations in surface water and groundwater suggest significant discharge of regional groundwaters into lowland rainforest watersheds (Genereux et al. 2002; Genereux and Pringle 1997; Pringle et al. 1993) which is supported by physical hydrologic data (Genereux et al. 2005) and ^{18}O data (Genereux 2004). This prior work has led to the development of a two endmember "conceptual hydrologic model" in which hydrology and water quality of this lowland rainforest study site is largely controlled by mixing of two distinct groundwaters: one young and recharged locally and the other much older, representing IGF, from a distant higher-elevation recharge area. If this model is correct than IGF accounts for more than half of the water and >90% of the major ions exported from some of the lowland watersheds and present in some lowland riparian wetlands (Genereux et al. 2005; Genereux et al. 2002).

The work described here uses radio-active isotope tracers (^{14}C and ^{36}Cl) and, to a lesser extent, stable isotope tracers (^{18}O) to test two key elements of the conceptual hydrologic model:

1) Tracer concentrations in shallow groundwater, springwater, and (for non-volatile tracers) streamwater are consistent with mixing of two distinct end-member waters (except for samples representing end-members themselves).
2) Bedrock groundwater involved in IGF has a much greater age than local water.

Data were also collected on CFCs, SF_6, and other trace gases; these dissolved gas data are an important part of the overall study but are not included in this thesis (another

graduate student is working with them). Because of extensive prior work on IGF at La Selva it is an excellent laboratory in which to test the utility and consistency of tracer data in identifying and quantifying mixing between groundwaters of very different age in a discharge area for IGF. The conceptual model involving IGF (based on major ion, physical hydrologic, and ^{18}O data) will be tested with data obtained on different tracers that have different source functions, behavior, and abilities (with respect to what they can constrain, identify, and describe).

A more thorough understanding of IGF has significance beyond this study. A better understanding of water and chemical fluxes into and through watersheds can provide a better understanding of biogeochemical processes and solute transport. IGF may also significantly influence wetland and aquatic ecosystems including effects on species diversity, rates of algal growth, and microbially mediated decomposition of organic matter (Rosemond et al. 2001; Ramirez 2000; Pringle 1993). This study also illustrates the importance of regional, rather than local, land/water use planning and conservation. Changes in land-use in the recharge area, such as development and/or deforestation may reduce or contaminate the regional groundwater system supplying IGF, affecting quantity and quality of water discharged in the distant lowland watersheds. Groundwater withdrawals from a regional groundwater system discharging in the lowlands could have unintended effects on lowland watersheds. The connection between regional groundwater systems and lowland watersheds is a relatively unexplored and potentially significant factor in the further understanding of regional hydrology as well as, in this case, the conservation of sensitive ecosystems such as lowland rainforest. The

information gained here is relevant towards better understanding and management of these areas.

Chapter 2. Background

2.1 Carbon-14

^{14}C is a naturally occurring radioactive isotope of carbon which decays by beta emission (emission of an electron or positron) with a half-life of 5730±40 years (Geyh and Schleicher 1990). It's produced as cosmic rays constantly bombarding Earth strike the upper atmosphere and produce thermal neutrons (having only the potential energy imparted by the ambient temperature). The thermal neutrons react with ^{14}N to produce ^{14}C (Kalin 2000):

$$^{14}N + n \rightarrow {}^{14}C + {}^{1}H \qquad \text{(Eq. 2.1)}$$

The ^{14}C produced in this reaction is quickly oxidized to $^{14}CO_2$ which mixes into the lower atmosphere. Any material using atmospheric CO_2 (plants), or reacting with atmospheric CO_2 (water) is going to have a ^{14}C activity equal to atmospheric ^{14}C while in equilibrium with the atmospheric carbon reservoir (Pearson and White 1967). ^{14}C generally enters the hydrologic cycle through four dominant pathways; dissolution of atmospheric CO_2 into rain water and surface water, plant respired CO_2 in the soil zone that dissolves into water, CO_2 resulting from oxidation of organic material in the soil that dissolves into water, and dissolution of mineral phases containing geologically young carbon (Kalin 2000).

Libby et al. (1949) were the first to report on the worldwide uniformity of ^{14}C in the biosphere and the potential for dating carbonaceous material. Many investigators have since shown that ^{14}C activity has not been constant over time, but has fluctuated due to changes in Earth's magnetic dipole moment, solar variability, and fluctuations in sunspot cycles (Geyh and Schleicher 1990). However, the effects from these factors are

relatively small and the internationally accepted value of modern ^{14}C activity has been set at 13.56 decays per minute per gram of carbon, the zero-year for this activity is 1950 A.D. This value is considered to represent 100 "percent modern carbon" (pmc) (Kalin 2000). Samples with a ^{14}C activity lower than this are pre-1950 A.D. After 1950, atmospheric nuclear weapons testing increased the amount of ^{14}C in the atmosphere, therefore samples with a ^{14}C activity greater than 100 pmc are post-1950 AD (Kalin 2000).

The ^{14}C age of groundwater refers to the time that has elapsed since the water was isolated from modern carbon in the unsaturated zone. ^{14}C ages are determined by comparing the ^{14}C activity of a sample to an initial activity and calculating a time using the following decay equation (Fontes and Garnier 1979):

$$t = \left(\frac{5730}{\ln 2}\right) \ln\left(\frac{A_0}{A_t}\right) \qquad \text{(Eq. 2.2)}$$

"t" is the time in years since the material was separated from the modern carbon reservoir (since the water was isolated from the unsaturated zone), "A_0" is the specific ^{14}C activity (grams of ^{14}C per gram of C) at time equal to zero, and "A_t" is the ^{14}C activity after a time t (the present ^{14}C activity of the material).

^{14}C activity, and ^{14}C dating, of groundwater can be affected by additions of and/or reactions with carbon bearing minerals and organic phases. There are four processes of particular interest with respect to ^{14}C dating of groundwater; dissolution of carbonate minerals such as limestone with 0 pmc can increase the concentration of DIC (dissolved inorganic carbon) while decreasing the ^{14}C activity of the DIC (e.g., Plummer and Sprinkle 2001), organic matter oxidation with 0 pmc can increase the concentration of DIC while decreasing the ^{14}C activity of the DIC (e.g., Aravena 1995), sorption of Ca and

Mg ions to mineral surfaces may cause the dissolution of carbonate minerals (e.g., Plummer et al. 1990), and carbonate recrystallization (dissolution and subsequent precipitation of the same mass of carbonate mineral) results in an isotope effect (Kendall and Caldwell 1998) causing the DIC to have a higher $\delta^{13}C$ and a lower ^{14}C activity (e.g., Parkhurst and Plummer 1983).

^{14}C dating of groundwater requires a quantification of the processes described above in order to determine the ^{14}C activity of DIC derived from atmospheric CO_2 at the time of isolation of the groundwater from modern carbon in the atmosphere. There are several models to correct ^{14}C activity for the effects of the processes listed above. Most use $\delta^{13}C$ and the major chemical constituents in groundwater to determine A_0. The most widely used "formula based" models of this type are the Ingerson and Pearson (1964), Tamers (1975), and Fontes and Garnier (1979) models.

Ingerson and Perason (1964) use a carbonate dissolution model to estimate initial ^{14}C activity in DIC based on $\delta^{13}C$ data for the inorganic carbon system, assuming that all DIC is derived from soil zone CO_2 and solid carbonates (Plummer et al. 1994). A_0 is determined by the proportion to which each of these sources contributes to the DIC of the groundwater sample. These proportions are determined by $\delta^{13}C$ data. This model can accurately correct for dissolution of carbonate minerals, and the resulting dilution of ^{14}C activity. Its main disadvantages are that the model requires inputs that can be difficult to obtain and must often be assumed, such as the $\delta^{13}C$ of soil CO_2, and it does not consider the effects of geochemical reactions other than mineral dissolution, particularly isotope exchange reactions.

The Tamers (1975) model is a mass balance model. The mass balance is performed only on carbonates and CO_2 gas and is based on chemical concentrations rather than $\delta^{13}C$ (Plummer et al. 1994). The dissolution of solid carbonates dilutes ^{14}C activity by the reaction of dissolved CO_2 with solid carbonate to form HCO_3^-.

$$H_2CO_3 + CaCO_3 \rightarrow 2HCO_3^- + Ca^{2+} \quad \text{(Eq. 2.3)}$$

In this reaction, half of the HCO_3^- results from solid carbonate and the other half is derived from CO_2 dissolved in the water sample at the time of recharge. This model is most applicable when the groundwater pH is near neutral and the above reaction is the dominant reaction affecting carbon chemistry. It corrects for the dissolution of solid carbonate, but not the effects of isotope exchange. The simplicity of the model makes it easy to use at the cost of limiting its capabilities and it can be conveniently modified to suit site-specific conditions (Kennedy 2004).

The Fontes and Garnier (1979) model is a hybrid of the Ingerson and Pearson (1964) model and the Tamers (1975) model, combining both chemical and isotopic data to correct for reaction effects on ^{14}C activity. The model considers a two-stage evolution of recharge waters accounting for dissolution and isotopic exchange with carbonate rocks in the saturated zone using a chemical mass balance similar to Tamers with a provision for base exchange (Plummer et al. 1994). The Fontes and Garnier model is the most widely used of the formula based models.

NETPATH is a computer mass balance program used to interpret net geochemical mass-balance reactions between an initial and final water along a hydrologic flow path. In addition to considering all carbon, organic and inorganic, it differs from the above models in that it determines A_0 and the correction for reaction effects on A_0 separately,

where the models mentioned above treat them in a single step. NETPATH first estimates A_0 for initial water by accounting for reaction effects in the recharge area only. Then a separate calculation is made that accounts for the reaction effects (mass transfers) that occur between the upgradient initial water and the downgradient final water. These mass transfers are then applied to A_0 to calculate A_{nd}, the ^{14}C activity the final water would have in the absence of radioactive decay (Plummer et al. 1994). A_t and A_{nd} are then used in the radioactive decay equation to calculate the age of the final water (Plummer et al. 1994):

$$t = \left(\frac{5730}{\ln 2}\right) \ln\left(\frac{A_{nd}}{A_t}\right) \qquad \text{(Eq. 2.4)}$$

The mass balance approach of NETPATH is generalized by the equation (Plummer et al. 1994):

initial water + reactant phases → final water + product phases (Eq. 2.5)

where "initial water" and "final water" refer to the water chemistry measured at an initial upgradient well and a final downgradient well, and the terms "reactant phases" and "product phases" refer to constituents that enter or leave the aqueous phase as the water flows from the initial well to the final well (Plummer et al. 1994). The mass balance problem in equation 3.5 is solved by using defined constraints and phases. A "phase" is any mineral or gas that can enter or leave the aqueous solution along the evolutionary flowpath. The selected phases should be known to occur in the system, even if in trace amounts (Plummer et al. 1994). The purpose of a constraint is to estimate the masses of phases that have entered or left the aqueous solution by dissolution, precipitation, or other geochemical reactions. A constraint is typically a concentration of a particular element or electrons (redox state) in the groundwater (Plummer et al. 1994). NETPATH was used in

this study to estimate the age of groundwater at Guacimo Spring, a large spring in the study area.

2.2 Carbon-13

^{13}C is a naturally occurring stable isotope of carbon that is useful in providing information about the origins of the DIC in water. $^{13}C/^{12}C$ data are reported as $\delta^{13}C$, relative to the PDB (Pee Dee Belemite) or the equivalent VPBD (Vienna Pee Dee Belemite) standard in parts per thousand, or per mil (‰) (Kendall and Caldwell 1998):

$$\delta^{13}C = \left[\frac{R_x}{R_{std}} - 1 \right] \times 1000 \qquad \text{(Eq. 2.6)}$$

where R_x and R_{std} are the $^{13}C/^{12}C$ ratio of the sample and standard respectively.

The utility of ^{13}C is a result of isotope fractionation. Isotope fractionation occurs because various isotopes of an element have slightly different chemical and physical properties resulting from their differences in mass. Strengths of chemical bonds involving different isotopic species will usually be different, bonds including heavier isotopes being harder to break than those including lighter isotopes (Kendall and Caldwell 1998). For elements of low atomic numbers, these differences are large enough for many physical, chemical, and biological processes or reactions to fractionate, or change, the relative proportions of different isotopes of the same element in various compounds (Kendall and Caldwell 1998).

Isotope fractionations can be either equilibrium or kinetic fractionations. Equilibrium fractionation is a result of reactions in which the forward and backward reaction rates are identical to each other. The heavier isotopes generally preferentially accumulate in the more dense material, such as ^{18}O in liquid water when the equilibrium

in question is between liquid water and water vapor (Kendall and Caldwell 1998). Kinetic fractionations are a result of reactions that are considered unidirectional such as many biological reactions or an otherwise equilibrium reaction in which the reactants become isolated from the products. In kinetic processes, the lighter of two isotopes of an element will form the weaker and more easily broken bond. Therefore the lighter isotope is more reactive, and becomes concentrated in reaction products, enriching the residual reactants in the heavier isotope (Coplen et al. 2000). As a result of fractionation processes $\delta^{13}C$ compositions of various components of the global carbon reservoir generally fall within distinct ranges (Table 2.1).

Table 2.1 – Typical $\delta^{13}C$ values from various sources.

Material	Average $\delta^{13}C$ (‰)	Reference
Atmospheric CO_2	-7.0 ± 0.6	Keeling (1958), Friedli et al. (1986), Francey et al (1999)
Marine limestone	-0.2 ± 2.8	Keith & Weber (1964), Plummer & Sprinkle (2001)
Sedimentary organic carbon and petroleum	-28 ± 4	Craig (1953)
Land plants	-25 ± 4	Craig (1953), Deines (1980)
Soil CO_2		
temperate climate (dominated by C_3 plants)	-21.1 to -28.0	Galimov (1966), Broecker and Olson (1960), Cerling et al. (1991)
arid climate (dominated by C_4 plants)	-16.7	Kunkler (1969), Deines (1980)
Mantle derived carbon	-5 to -8	Pineau & Javoy (1983), DesMarais & Moore (1984)

The $\delta^{13}C$ composition of dissolved inorganic carbon (DIC) in natural waters is controlled by the sources and sinks of carbon described in section 2.1 and results from the fractionation between solid phases, dissolved phases, gaseous phases, and oxidation states. Typically the major sources of carbon contributing to DIC in natural waters are atmospheric CO_2, CO_2 from the oxidation of organic matter, and carbon from the dissolution of carbonate minerals (Tan 1989). In the context of the NETPATH and the other ^{14}C geochemical models described in section 2.1, $\delta^{13}C$ is used to determine the extent to which the sources and sinks have influenced ^{14}C activity of groundwaters, making it possible to separate the effects of the decay of ^{14}C from other processes.

2.3 Chlorine-36

^{36}Cl is a naturally occurring radioactive isotope of chlorine. It has a half-life of 301,000 ± 4,000 years and decays by beta emission (Lin et al. 2005). ^{36}Cl values are typically reptorted as the ratio of ^{36}Cl to total Cl multiplied by 10^{15} ($^{36}Cl/Cl \times 10^{15}$). It is produced in the atmosphere, at Earth's surface, and in the deep subsurface by spallation reactions and neutron activation (Bentley et al. 1986a). Spallation reactions result from cosmic ray particles colliding with the nuclei of terrestrial atoms, causing them to emit a number of energetic neutrons and protons, and leaving one large residual nuclear mass. After emission of additional particles to lower the energy of the excited nuclear mass, a new stable or long-lived radioactive nucleus results (^{36}Cl) (Phillips 2000). Neutron activation refers to the capture of thermal neutrons by the nuclei of an atom (Phillips 2000).

^{36}Cl is produced in the atmosphere by spallation of ^{40}Ar and neutron activation of ^{36}Ar. About 40% of atmospheric ^{36}Cl production occurs in the troposphere (the layer of the atmosphere nearest Earth's surface) and 60% occurs in the stratosphere. Stratospherically produced ^{36}Cl enters the troposphere during periods of mixing (Bentley et al. 1986a). The troposphere also contains stable chloride from sea spray; the mixture of ^{36}Cl and stable chloride is quickly rained out of the troposphere or becomes associated with aerosols which also fall out quickly (mean residence time of 1 week). The fallout of chloride decreases exponentially from the coastal areas toward continental interiors (Bentley et al. 1986a).

^{36}Cl produced at, and within the first few meters of, Earth's surface (epigene zone) by spallation of K and Ca and neutron activation of ^{35}Cl, is the major source of ^{36}Cl in the first few meters of the Earth's surface and the ocean. Buildup of ^{36}Cl from cosmic ray processes begins as soon as a rock is exposed at the surface of the earth (Bentley et al. 1986a). ^{36}Cl produced in this manner may be released through weathering and allowed to enter the hydrologic cycle (Bentley et al. 1986b). In the deep subsurface (hypogene zone) the dominant source of ^{36}Cl is neutron activation of ^{35}Cl associated with the decay of U and Th isotopes. In this zone the $^{36}Cl/Cl$ ratio eventually arrives at a secular equilibrium reflecting the balance between production rate and decay of ^{36}Cl. Because production is dependant on neutron flux, ^{36}Cl is not only produced in the rocks of the subsurface, but also anything residing within or moving through them (i.e., groundwater) (Rao et al. 1996).

Because of the conservative behavior of Cl (under normal conditions it is neither precipitated nor sorbed) ^{36}Cl has proven to be a useful hydrogeologic tracer. Using ^{36}Cl

data in conjunction with ^{14}C data Purdy et al. (1996) developed a model to describe groundwater flow velocities in the Aquia Aquifer in Maryland based on changes in ^{36}Cl concentrations of meteoric water with distance inland from the ocean and changes in the location of the coastline since the Pleistocene. The model highlighted different flow velocities, likely resulting from different hydraulic gradients, between the upper and lower portions of the aquifer. This study also brings to light the potential influence that climatic factors (and their variability) such as global production rates, rise and fall in sea level, and concentration of Cl in precipitation can have on ^{36}Cl concentrations and $^{36}Cl/Cl$ ratios in recharge water.

^{36}Cl decay has been used to date very old groundwater in the Milk River Aquifer in Alberta, Canada (Phillips et al. 1986), and the Great Artesian Basin, Australia (Bentley et al. 1986b; Torgersen et al. 1991) and was found to be useful where the geochemistry and groundwater flow characteristics were relatively simple and straightforward. The major complication in these studies was is in determining the initial $^{36}Cl/Cl$ ratio and the effects of the geochemical evolution since recharge.

^{36}Cl has also been used as a tracer in studies of geothermal waters (Phillips et al. 1984; Fehn et al. 1992; Rao et al. 1996). Under geothermal conditions, chloride can be leached from rock formations in amounts sufficient to "tag" the waters passing through them with a $^{36}Cl/Cl$ ratio characteristic of that formation. Fehn et al (1992) used $^{36}Cl/Cl$ and Cl concentration data in conjunction with ^{129}I data to distinguish between groundwaters of different origin (meteoric and formation), as well as determining their residence times based on the build-up of ^{36}Cl and ^{129}I in the Clear Lake area of California. Rao et al. (1996) and Phillips et al. (1984) used ^{36}Cl data to determine the

major source formations of chloride in hydrothermal waters, giving information on the depth of groundwater circulation.

2.4 Oxygen-18

^{18}O is a naturally occurring stable isotope that has been used extensively in hydrologic investigations (Coplen et al. 2000). $^{18}O/^{16}O$ data are reported relative to Standard Mean Ocean Water (SMOW) or Vienna Standard Mean Ocean Water (VSMOW) in parts per thousand or per mil (‰) (Kendall and Caldwell 1998):

$$\delta^{18}O = \left[\frac{R_x}{R_{std}} - 1 \right] \times 1000 \qquad \text{(Eq. 2.7)}$$

where R_x and R_{std} are the $^{18}O/^{16}O$ ratio of the sample and standard respectively.

The value of ^{18}O as a tracer is a result of the change in isotopic composition of precipitation resulting from fractionation (see section 2.2) that can be attributed to a number of factors. Of particular interest in this study are the "altitude effect" and the continental effect. The "altitude effect" refers to the decrease in ^{18}O concentration in precipitation with increase in altitude on the windward side of a topographic barrier, such as a mountain range, because of isotopically heavier water molecules preferentially raining out. The magnitude of the altitude effect depends upon local topography and climate (Coplen et al. 2000), and has been estimated to be about 1.9‰ per kilometer of elevation in the area of Costa Rica in which our study site is located (Lachniet and Patterson 2002). The "continental effect" refers to the decrease in ^{18}O concentration in precipitation inland from the coast due to removal of moisture from air masses as they are orographically uplifted during inland movement (Coplen et al. 2000).

Because of these two processes ^{18}O data can be applied to problems in hydrology including hydrograph separation (Laudon et al. 2002; Genereux and Hooper 1998; Harris et al. 1995; Ribolzi et al. 1996; Eshleman et al. 1993) and estimation of recharge (Herczeg and Edmunds 2000; Coplen et al. 2000; Gonfiantini et al. 1998; Wood and Sanford 1995). ^{18}O data has also been used to separate out the fractions of different types of water derived from different source locations outside of a single watershed. Muir and Coplen (1981) conducted an investigation using $\delta^{2}H$ and $\delta^{18}O$ data to calculate the fractions of imported northern California water and local groundwater in pumped well water samples in the Santa Clara Valley, CA. Thyne et al. (1999) used ^{18}O data with other tracer data to calculate the volume of interbasin groundwater flow (groundwater recharged from at a different geographic location) which flow through faulted and fractured bedrock in the southern Sierra Nevada.

Chapter 3. Study Site

3.1 Location and area

La Selva Biological Station is 1536-ha research and education preserve owned and operated by the Organization of Tropical Studies (OTS) (Figure 3.1). It's located in the province of Heredia at the confluence of Rio Sarapiqui and Rio Puerto Viejo (McDade and Hartshorn 1994). La Selva is at the down slope end of a tract of rainforest that extends through Braulio Carrillo National Park and up the north slope of Volcan Barva, about 35 km to the south (Figure 3.2).

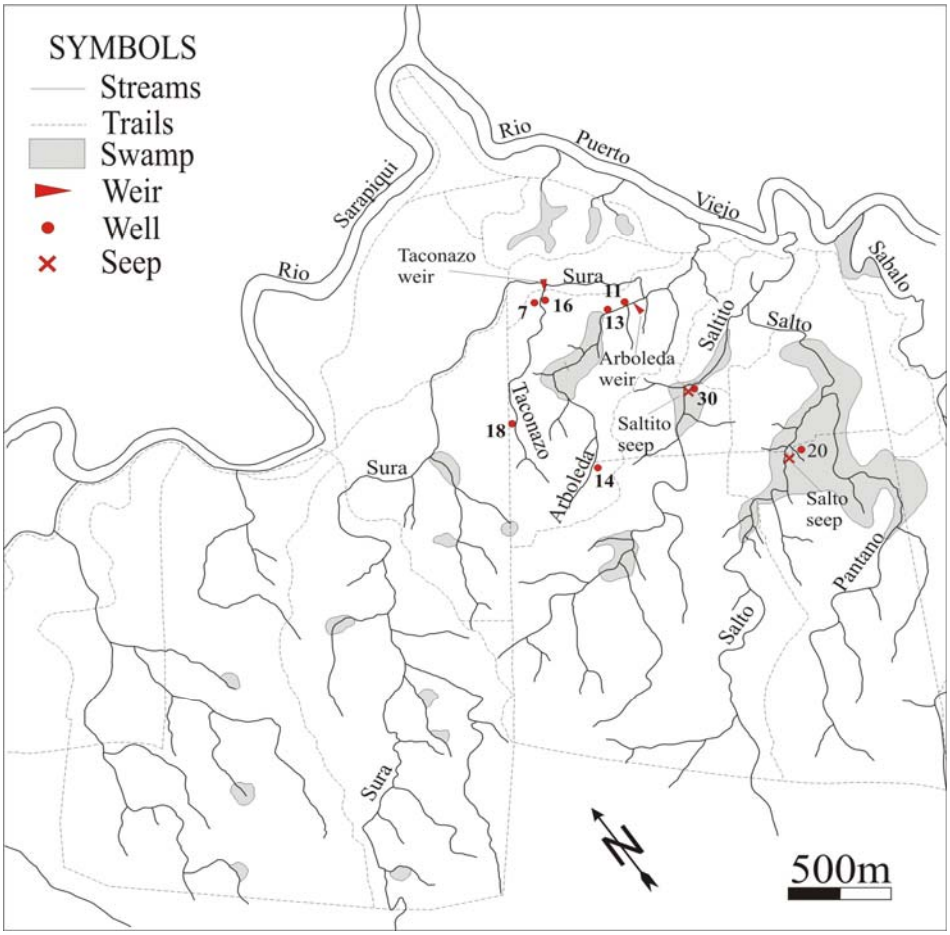

Figure 3.1. Map of La Selva Biological Station.

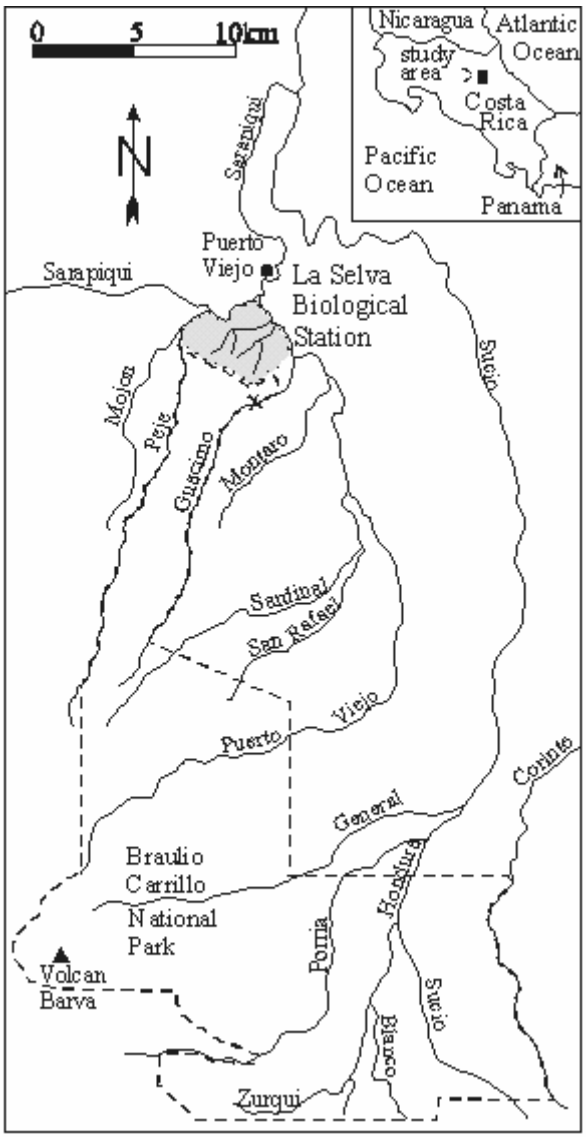

Figure 3.2. La Selva Biological Station with respect to Braulio Carrillo National Park and Costa Rica

The elevation at La Selva ranges from 35 meters above sea level along Rio Puerto Viejo to 137 meters above sea level at the southwest corner of the preserve (McDade and Hartshorn 1994). The topography ranges from relatively flat terraces along the rivers to steep undulating hills to the south and southwest.

3.2 Climate

La Selva is a tropical rainforest. The average annual precipitation from 1958 to 2004 was 4260 mm per year, with a high in 1970 of 6067 mm and a low in 1985 of 3129 mm (http://www.ots.duke.edu/en/laselva/metereological.shtml). Average monthly precipitation is bimodal with peaks of more than 400mm per month in June-July and November-December and the period of lowest rainfall from February to April (March being the driest) (Sanford et al. 1994).

The average annual temperature at La Selva is 25.8ºC. La Selva is typical of the tropics with respect to temperature in that the daily range of temperature (6-12˚ C) is much greater than the range of average monthly temperatures (< 3˚ C) (Sanford et al. 1994).

3.3 Vegetation

Hartshorn and Hammel (1994) divided land cover at La Selva into seven categories: primary forest (55%), moderately high-graded forest (7.4%) ("high-graded" refers to a type of timber harvesting in which trees of the highest value and quality are harvested and the others of less value are left), secondary forest (10.6%), early successional pasture (17.7%), abandoned plantations (7.5%), arboretum and managed habitats (0.5%), and developed areas (1.1%). All of the sampling locations for this study fall in the primary forest category except well 11, well 13, and Arboleda weir, which fall in the arboretum and managed areas category.

The primary forests are dominated by *Pentachlethera Macroloba* which forms the base of the canopy at 30-35m high. A variety of species of lesser importance are

scattered throughout, some reaching 50-55m of height. This gives the canopy an irregular topography. Swampy areas such as those along the Sura, Salto, and Arboleda streams have a slightly different vegetation type. *Pentachlethera* is still the dominant canopy species, but several other species are characteristic to these areas such as *Carapa nicaraguensis*, *Luehea seemannii* Triana and Planchon (Tiliaceae), and *Otoba novogranatensis* Moldenke (Myristicaceae) (Hartshorn and Hammel 1994).

The arboretum and managed habitats land use category includes the Holdridge Arboretum (location of well 11, well 13, and Arboleda weir). This area is a 3.5 ha patch of former cacao plantation. In 1968 the cacao was removed and the area now has over 1,200 trees of over 250 native species (Hartshorn and Hammel 1994).

3.4 Geology

Located on the Caribbean side of the volcanic mountain chain that makes up the Cordillera Central, about 35 km north of Volcan Barva, La Selva Biological Station sits near the western edge of a large region called the Limon Basin (Cuenca de Limon) which occupies northeastern Costa Rica and is bounded by volcanic mountain chains to the southwest, the Rio San Juan along the Nicaraguan border, and the Caribbean coast (Weyl 1980). This area is a southeastern continuation of the Nicaragua Depression and is a sedimentary basin dating back to the early Tertiary (Weyl 1980). It's covered by alluvium from numerous rivers. At the foot of the volcanoes this alluvium takes the form of fans and lahar deposits. The combined thickness of the sediments in the Limon Basin reaches more than 10,000 m (Weyl 1980).

Rymer et al. (2000) described Volcan Barva and Volcan Poas as standing on upper Tertiary pyroclastic avalanche deposits, which in turn lie unconformably on the "intra-canyon lavas" of the Aguacate formation. The Aguacate has been mapped throughout western and central Costa Rica (Weyl 1980), but whether the Quaternary volcanics described at La Selva (below) are on top of the Tertiary deposits of the Limon Basin, or the 900 m thick Aguacate formation (Weyl 1980), is unknown. From the log of a water supply well drilled at La Selva it is known that volcanic lithology persists for at least 50 m beneath the surface near the dining hall and administrative offices of the research station.

Alvarado (1990) described La Selva's location as at the edge of the volcanic arc and the back arc basin. The surficial geology of the land in the general vicinity of La Selva is dictated by ash falls, lahars, and lava flows. At La Selva, ash falls and lahars have played only a minor role in building the land surface (Sollins et al. 1994). The geology is composed mainly of three Quaternary (Pleistocene) lava flows from Volcan Barva recognized by Alvarado (1990) from scarce outcrops, lithic fragments in the soil, and cobbles and boulders in the streams. The following discussion is based on his work.

Alvarado (1990) found the Vargas basalt to be the oldest of the three lava units. The exact thickness of this unit is unknown, but it is known to be at least 2 m. It's slightly alkaline in composition and low in Mg. Weathered surfaces appear brown to brown-orange in color, fresh surfaces are light gray. Alvarado (1990) described the texture as porphyritic-hypocrystalline. Plagioclase phenocrysts account for 10-18% of the rock (some as large as 2 cm in length). Olivine phenocrysts, some of which show alteration to serpentine and iddingsite, make up of 1-1.5% of the rock unit. About 79-85% of the rock

is composed of matrix made up of brown glass, microlites of plagioclase, clinopyroxene, opaque minerals, and trace olivine. Vesicles comprise 0.5-1.5% of the rock unit. Chlorite, serpentine, zeolite, and oxides of iron were found filling the fractures.

The Salto basaltic-andesite is intermediate in age and overlies the Vargas basalt. Its thickness increases to the south up to 55m. It's defined as a pyroxene andesite with olivine and is light gray to black in color. Plagioclase phenocrysts (up to 3 cm in size) constitute 10-25% of the rock. Olivine phenocrysts, some of which are partially altered to iddingsite, serpentine, and occasionally calcite, make up 2.5-4.5% of the rock unit. Clinopyroxene phenocrysts, sometimes having inclusions of magnetite, plagioclase, or olivine, comprise 2.5-4.5% of the rock unit. Orthopyroxene and magnetite phenocrysts make up 0-2% and 0-3% of the rock unit respectively. The matrix making up 65-80% of the rock unit is composed of microlites of plagioclase, orthopyroxene, opaques, and occasionally olivine. Vesicles make up 0-3% of the rock unit.

The Esquina andesite is the youngest of the three lava units recognized by Alvarado (1990). Radiometric dating estimates that it was emplaced in the lower Pleistocene at 1.2 Ma. Its thickness averages 20 m, although it may surpass 35 m, and it overlies the previous two units. It appears dark gray to black, but when weathered can appear gray to brown and be easy to confuse with tuff. Phenocrysts of plagioclase comprise 1.5-3.5% of the unit, phenocrysts of clinopyroxene, orthopyroxene, and opaque minerals comprise 0.5-3%, 0-1.5%, and 0-1.5% of the unit respectively. Vesicles make up 0-4% of the rock unit.

Fluvial and palustrine (swamp) deposits cover a part of La Selva as well. Fluvial deposits are made up of interstratified sand and volcanic mud with conglomerate and iron

mud intercalations. Their thicknesses vary from a few centimeters to a few meters. Some recent palustrine deposits are also present. They develop in swamps in soils rich in organic material, mud, and clay. The maximum thickness of these deposits rarely exceeds 1 m and is usually between 10 and 40cm.

3.5 Hydrogeology

There has been no scientific drilling on the north side of Volcan Barva. What is known about the hydrogeology of this area is inferred from work that has been done on the more populous south side of Volcan Barva by Parker et al. (1988) and Foster et al. (1985) where groundwater is an important resource for the Valle Central. Similar characteristics can be expected on the north side.

As described above, this area is characterized by Quaternary lava flows. It's these andesitic and basaltic lavas that function as aquifers. They have high transmissivity with groundwater flow concentrated through high permeability horizons associated with breccias or well fractured parts of the lava flows (Parker et al. 1988). Recharge occurs through surface infiltration with subsequent downward transfer between lava layers and by leakage directly to lavas where they are exposed along river valleys (Parker et al. 1988). While there is no direct evidence for volcanic tuffs at La Selva (Sollins et al. 1994) tuffs are present on the south side of Barva and play a significant role in groundwater recharge, storage, and transfer between lava flows because of their porosity (45-64%) and hydraulic conductivity (0.02-0.5 m/d) (Parker et al. 1988).

3.6 Soils

Soil formation at La Selva is primarily related to three processes: in-place weathering of the volcanic materials previously described, fluvial processes in areas adjacent to the rivers and streams, and accumulation of organic material in the poorly drained areas (Sollins et al. 1994). At La Selva many soil consociations have been described, however all the sampling locations in this study lie in four types, the Jaguar, the Arboleda, the Taconazo, and the Complejo de Pantano (Table 3.1).

Table 3.1. Sampling locations and soils they reside in.

Sampling location	Soil type
Well 11	Arboleda
Well 13	Arboleda
Well 14	Arboleda
Arbo weir	Arboleda
Well 16	Jaguar
Well 7	Jaguar
Well 18	Taconazo
Taco weir	Jaguar
Well 20	Complejo el Pantano
Salto seep	Complejo el Pantano
Well 30	Complejo el Pantano
Saltito seep	Complejo el Pantano
Guacimo Spring	not mapped

The Jaguar soil consociation is the second most extensive consociation at La Selva and occupies the central portion of the property. It's derived directly from the Esquina andesite. These soils are strongly acidic, rich in organic matter, and highly leached. They also have a low degree of base saturation (30%) and a fairly large amount

of exchangeable acidity (Sollins et al. 1994). These soils are classified as a Typic Tropohumult.

The Arboleda was long thought to be derived from the Esquina andesite, now it's believed to be an alluvial soil from an old river terrace. This soils series is generally acidic, and is classified as a Typic Humitropept (Sollins et al 1994).

Hydrologically, the Arboleda and Jaguar soil consociations are known for their aggregation. The aggregates surround large macropores, which are formed as a result of root decay and soil animals (Sollins et al. 1994). Water flows through these macropores and bypasses the micropores of the soil matrix. Nutrients in the soil matrix therefore tend not to leach. Solute exchange studies done on the Helechal soil consociation (having similar aggregation characteristics as the Jaguar and Arboleda soil consociations) by Sollins and Raudulovich (1988) found that large amounts of water (greater than two pore volumes) must flow through the soil to completely leach nutrients from the fine pores.

The Taconazo soil consociation is found along the central and southern portion of the Taconazo stream, which roughly corresponds to its parent material, the Vargas basalt. The surface soil is base poor and strongly acidic. Below 22cm the soil appears gray in color indicating poor drainage, and in places the water table rises to within 50 cm of the surface. The dominant soil type is Typic Tropoquept.

The Complejo El Pantano (the swamp complex) soil consociation is found in some of La Selva's swampy depressions. High water tables in these areas have caused reducing conditions and subsequent accumulation of organic matter; as a result they are typically gleyed and mottled (Sollins et al. 1994). All these soils are classified as Tropoquepts; Histic Tropoquepts where the water table is often above the soil surface,

Typic Tropoquepts where the water table remains lower, and Lithic Tropoquepts where the streams have cut the valley floor down to the bedrock (Sollins et al. 1994).

3.7 Geomorphology

La Selva sits in a transition zone between the foothills of the Cordillera Central and the Caribbean coastal plain. It straddles two geomorphic provinces that Alvarado (1990) referred to as the La Selva irregular hills and the fluvial terraces.

The morphology of the La Selva irregular hills is a product of the accumulation of irregular lava flows that have been weathered and eroded since the middle Quaternary. There is a general slope to the land of about 2-3˚ to the northeast, in possible correspondence with the lava flows. (Alvarado 1990)

At lower elevations fluvial processes have also played a role in shaping the landscape of La Selva, depositing alluvium and forming terraces along the Rio Puerto Viejo and Rio Sarapiqui (Sollins et al. 1994). Alvarado (1990) recognized five terraces. The Arboleda soil consociation, present in the northern portion of the Arboleda watershed (well 11, well 13, and the Arboleda weir), was probably formed from the uppermost terrace.

3.8 Water Quality and Hydrology

Stream chemistry at La Selva has been the subject of several studies. A study of stream nutrients initially identified the presence of solute rich waters in the Salto stream, particularly phosphorous (Pringle et al. 1986). Pringle et al. (1990) found large spatial variability in stream water chemistry in the Sura watershed (including the Arboleda,

Taconazo, and Salto streams) between 35 and 350 m above sea level. Phosphorous concentrations were found to be low in the Taconazo, streams above 350 m, and even streams whose entire drainage area included relatively high phosphorous soils. The processes that determine phosphorous concentrations were thought to be different from those that control nitrogen concentrations (spatial patterns in stream nitrogen were not similar to those in stream phosphorous).

Pringle and Triska (1991) suggested that the high phosphorous concentrations in the lowland streams of Costa Rica reflect the input of solute-rich geothermal waters. Pringle et al. (1993) explored similarities in water quality near three Costa Rican volcanoes (Barva, Poas, and Arenal) and the relationship between water quality and stream microbial ecology. Genereux and Pringle (1997) found that sodium and chloride concentrations of dry season water from 23 different stream sites at La Selva and one large spring nearby fell along a highly linear trend interpreted as a mixing line between two endmembers (Figure 3.4), suggesting that most of the large spatial variation in concentration among streams and riparian seeps could be explained by mixing of two distinct waters: high-solute "geothermal groundwater" and a low-solute "local water" (derived from precipitation onto, and draining from hillslopes within, the La Selva watersheds). The samples used to define geothermal groundwater were from Guacimo Spring, a large perennial spring on the northwestern bank of the Guacimo River about 1.5 km south of the southeastern corner of the La Selva boundary.

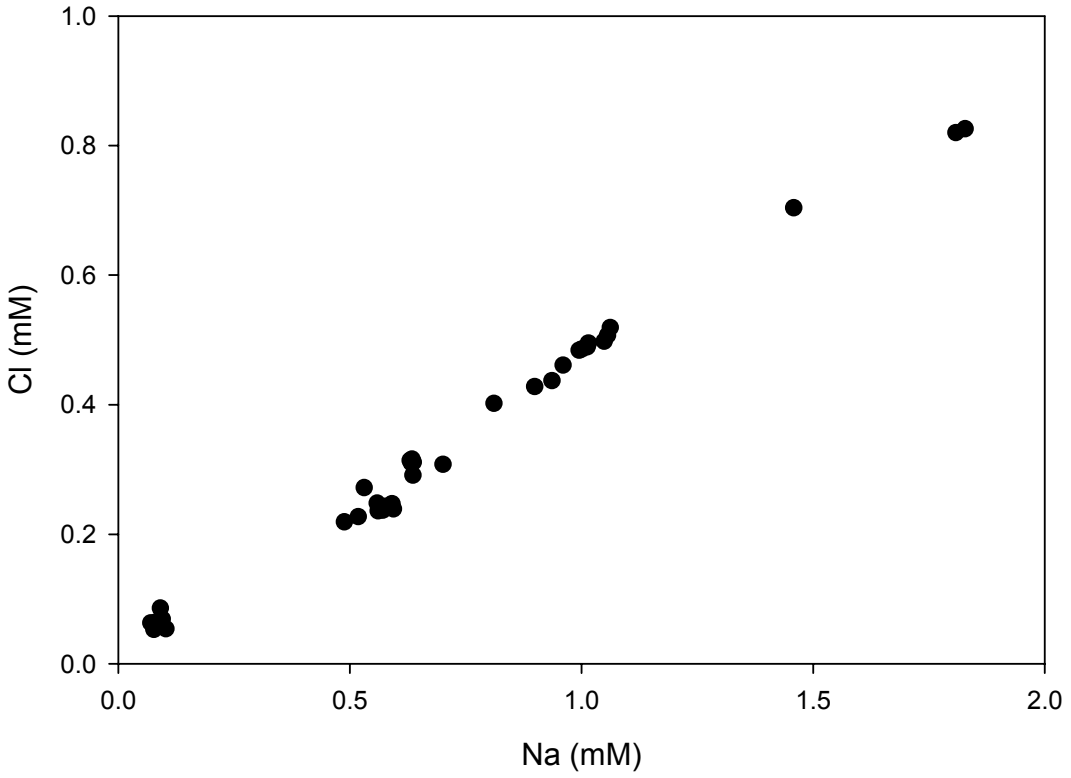

Figure 3.3. Na vs Cl from stream sites at La Selva Biological Station (Genereux and Pringle 1997)

Genereux et al. (2002) carried out further mixing model calculations with a much larger sample set that included both groundwater and surface water, and spanned 4.5 years. It was comprised of: (1) detailed dry season sampling (27 stream and riparian seep sites) in 1994, 1997, and 1998, (2) monthly stream and riparian seep samples at 9 sites from August 1993 to December 1997, (3) near stream groundwater samples from 25 wells from October 1993 to December 1994 (monthly) and March 1998, and (4) monthly Guacimo Spring samples from January 1995 to March 1998. Most of the variability in major ion concentrations in this larger sample set could, as with Genereux and Pringle (1997), be explained by mixing of two chemically and hydrologically distinct waters:

low-solute local water and high-solute "bedrock groundwater". The term "bedrock groundwater" was used instead of the earlier term "geothermal groundwater" to emphasize the geological medium in which the high-solute groundwater flow most likely occurs rather than geothermal processes or other possible controls on the chemistry of the water. A two-component mixing model that made it possible to calculate the fraction of water in a stream sample that is due to the discharge of bedrock groundwater was presented. Using this model the Taconazo stream was found to be virtually all local water and the Arboleda was found to exhibit mixing of bedrock groundwater and local water (average dry-season fraction of bedrock groundwater was 0.49).

The mixing model described above was further evaluated in Genereux (2004) using $\delta^{18}O$ data. The bedrock groundwater endmember was found to be both isotopically lighter and less temporally variable than the local water endmember, consistent with recharge from a higher elevation and flow through a regional groundwater system. This added further support to the idea that bedrock groundwater at La Selva (in the Arboleda, Sura, Salto, and other watersheds) represents interbasin groundwater flow (i.e. groundwater flow into La Selva beneath topographic divides, in a regional groundwater system). Some low elevation surface and groundwater sites at La Selva (including the stream and wells in the Arboleda watershed) were found to show significant contributions from both endmembers. $\delta^{18}O$ data could not be used to separate the two waters due to the high variability in $\delta^{18}O$ of the local water endmember.

Genereux et al. (2005) studied the interbasin groundwater flow at La Selva in the context of both physical and chemical watershed budgets. It was found that interbasin groundwater flow accounts for about 2/3 of water and 97% of major ion input to the

Arboleda watershed and interbasin groundwater flow was found to affect the Taconazo very little if at all.

Chapter 4. Methods

4.1 Field Methods

Water was collected from thirteen locations (well specifications in Table 4.1) in March 2006: three wells in the Arboleda watershed, three wells in the Taconazo watershed, one well and one seep in the Salto swamp, one well and one seep in the Saltito swamp, both the Arboleda and the Taconazo streams, and Guacimo Spring. In December 2006 two shallow groundwater samples (BCNP 1) were collected upslope of La Selva on the flanks of Volcan Barva at about 660 m elevation, in the possible recharge area for bedrock groundwater (Genereux 2004). Only the DIC, ^{14}C activity, and $\delta^{13}C$ data for one (BCNP 1) were available in time for inclusion in this thesis. The exact same methods were used for sample collection in March and December.

Table 4.1. Well information. "Installed" refers to the month the well was installed. "Depth" refers to the distance from the ground surface to the bottom of the PVC cap or plug at the bottom of the screen. "Screen" refers to the screened interval, in cm below ground surface. "Stick-up" refers to the distance from the ground surface to the top of the well cap above ground. "Water level" refers to the depth of the water level (below ground surface) just before the start of sampling in March 2006.

Well	Installed	Depth (cm)	Screen (cm)	Stick-up (cm)	Water level (cm)
11	Nov-05	207	145.5 - 177	14	82.5
13	Nov-05	165	99.5 - 131	26	42
14	Nov-05	119	67 - 98.5	52	35
16	Feb-06	198	119.5 - 151	35	87
7	Feb-00	121	76.5 - 108	28	92
18	Mar-06	128	76.5 - 108	44	25
20	Nov-05	129	79.5 - 101	42	86.5
30	Feb-06	102	56.5 - 88	70	15

Each well was purged until pH, dissolved oxygen (DO), temperature, and conductance were observed to be constant. At least three well volumes were purged even

if the water quality indicators stabilized before that. After purging, the samples were collected. Once all the samples were collected, they were transported by backpack to the lab. Samples were then transported back to the United States where they were shipped and/or delivered to the respective labs for analyses. Of the samples that were filtered, all except those to be analyzed for dissolved organic carbon (DOC) were filtered using an Aquaprep 600 cartridge filter, which has a 0.45 μm pore size and a hydrophilic polyethersulfone membrane. Samples analyzed for DOC were filtered with a 0.70 μm pore size glass fiber filter to prevent the introduction of DOC from the filter membrane.

Purging and sampling was done with a Series II Geopump from Geotech Environmental Equipment, a peristaltic pump designed for field sampling. Peristaltic pumps move fluid through a tube that's held stationary in a track by squeezing the tube with a moving set of rollers. As a roller squeezes the tubing closed, the fluid is forced ahead. When a closed section of tubing reopens, a partial vacuum draws the fluid through the tubing and the next roller traps more fluid, repeating the process (Atkinson, 1998). The tubing assembly consisted of a length of ¼ in OD x 3/16 in ID copper tubing (intake tubing), attached with a hose clamp to a 40 cm length of ¼ in ID Viton tubing in the pump head (pump and discharge tubing). The copper tubing was long enough to reach to the bottom of each well. Monitoring of pH, dissolved oxygen (DO), temperature, and conductance was done with a Sonde probe placed at the bottom of a 1 liter (1L) plastic bucket. The discharge tubing was place at the bottom of this bucket and water was allowed to overflow. The pumping rates at different sampling sites varied from about 30 to 300 milliliters per minute (ml/min) during purging and sampling (Table 4.2).

Table 4.2 -Sampling information. Temperature, dissolved oxygen, dissolved gases, and conductance values were measured by the Sonde probe once they were determined to be constant immediately before sampling. Values for major anions to dissolved trace gases refer to the order in which those samples were taken (e.g. for most sites, major anion samples first, major cation samples second, ^{18}O third, etc.). Blank spaces represent a parameter that was not measured or a sample that was not taken.

	sample location													
Parameters	**Well 11**	**Arbo weir**	**Well 13**	**Well 14**	**Well 16**	**Well 7**	**Well 18**	**Taco weir**	**GS**	**Well 20**	**Salto seep**	**Well 30**	**Saltito seep**	**BCNP1**
Date	3/5/06	3/5/06	3/6/06	3/6/06	3/7/06	3/7/06	3/8/06	3/8/06	3/9/06	3/10/06	3/10/06	3/11/06	3/11/06	12/14/06
Temperature (ºC)	25.01		24.53	24.39	24.64	24.48	24.46	23.96	25.44	25.25	25.02	24.44	24.31	
Dissolved oxygen (mg/L)	0.5		0.57	2.07	2.23	2.84	1.01	8.99	4.09	2.87	4.76	3.53	5.42	
Dissolved gases (mm of Hg)	733		734	757	764	764	748	741	781	757	769	775	732	
Specific conductance (µS)	350.2		160.8	15.0	1.0	12.3	35.3	7.8	624.1	455.0	484.1	62.2	180.6	
Major anions	1	1	1	1	1	1	8	1	1	7	1	1	1	1
Major cations	2	2	2	2	2	2	9	2	2	8	2	3	2	2
^{18}O	3	3	3	3	3	3	10	3	3	9	3	4	3	3
Alkalinity	4	4	4	4	4	4	11	4	4		4	5	5	4
pH	5	5	5	5	5	5	12	5	5	11	5	2	4	5
Ca-isotopes	6	10	6	6		6	13	6	6	10	6	6	6	
^{13}C	7	6	7	7	6	7	1	7	7	1	7	7	7	
^{14}C	8	7	8	8	7	8	2	8	8	2	8	8	8	7
^{3}H	9	8	12	9	9	11	3	9	9	5	9	9	11	8
DOC	10	9	9	10	8	9	4	10	10	6	10	10	9	6
CFCs	11		10	11	10	10	5	12	12	4	12	11	10	9
SF^6	12		11	12	11	12	6		13	3	13	13	13	10
^{36}Cl	13	11	13	13	12	13	7	11	14	12	14	14	14	11
Dissolved trace gases	14		14	14	13	14	14		11	13	11	12	12	12
Pumping rate (ml/min)	175	250	200	100	100	375	160	350	200	35	260	80	230	550

During purging the end of the intake tube was placed about 10 cm below the water level, and was moved downward as the water level dropped, being careful not to let the water level drop below the top of the screen. The volume of water purged from each well, and the overall rate of purging, was determined by timing how fast a bucket was filled with water pumped from the well. Purge volumes and times were recorded in a notebook in the field (as was the time, bottle rinse volume, and other information for each sample collected).

The same pump and filter system was used to collect the samples taken from the streams, seeps, and Guacimo Spring (without the purging process needed for wells). At the streams sites the intake tube (copper) was placed in the stilling pool just upstream of the V-notch weir. At the seep sites the intake tube was placed directly in the surface water from the seep (for the Salto seep, a small still pool, about 15 cm deep and 40 cm in diameter, in a depression on the bank of the Salto river; for the Saltito seep, a shallow rivulet about 5-10 cm deep and 50 cm wide whose point of origin was obscured by vegetation). At Guacimo Spring, samples were drawn from the rectangular concrete cistern that captures the spring outflow. Access was by a steel door, about 1 ft^2 in area, in the concrete roof of the cistern (the door farthest upgradient of the three doors). Water inside the cistern is free flowing along its long axis. In order to sample the spring, we reached the copper intake tube about 1.5 m into the cistern, in the up-gradient direction from the door. At these locations, at least three tube volumes of water were run through the tubing from intake to discharge in order to rinse out the tubing (this being taken care of by purging at the well locations).

Sample collection is described here in the order in which it occurred at most sampling sites, applies to each sampling site in the study except where otherwise noted, and includes samples taken for the analyses of CFCs, SF_6, ^3H, and trace gases (^3He, ^4He, Ne, Ar, Kr, N_2, O_2, CH_4, and various isotopes of Xe) (Table 4.2). Interpretation of the ^3H and trace gas data is part of the overall project but not part of this thesis. Sampling protocols were either provided in writing by the laboratories performing the analyses or developed from personal communications with technicians and researchers at the laboratories, information provided by those and other laboratories, and selected readings.

Two samples filtered to 0.45 μm were first collected from each site for the analysis of major anions (Cl^- and SO_4^{2-}). Samples were collected in 20 ml polyethylene vials. Each vial and cap was rinsed three times with filtered water from the sampling site immediately before the sample was collected. Special care was taken not to touch the inside of the neck of the vial or the inside of the cap.

Two samples filtered to 0.45 μm and acidified with 2N HNO_3 were collected for the analysis of major cations (Ca^{2+}, K^+, Mg^{2+}, Na^+). The samples were collected in 20 ml polyethylene vials. Each vial and cap was rinsed three times with filtered water from the sampling site immediately before the vial was filled to collect the sample. A small amount of water (several drops) was poured out of the vial to make room for the acid. 2 drops (about 100 μl) of 2N HNO_3 were added to the sample before it was capped.

Two samples filtered to 0.45 μm were collected for the analysis of ^{18}O. The samples were collected in 20 ml polyethylene vials. Each vial and cap was rinsed three times with filtered water from the sampling site immediately before the vial was filled to

collect the sample. Special care was taken not to touch the inside of the neck of the vial or the inside of the cap.

One sample filtered to 0.45 μm was collected for the measurement of alkalinity. The sample was collected in a 500 ml LDPE (low density polyethylene) bottle. The bottle was rinsed three times with filtered water from the sampling site immediately before the sample was collected. The bottle was then filled with about 150 ml of water. Measurement of alkalinity is described in the "Lab Methods" section.

Next, the filter was removed and pH was measured using an Oakton model "pH 11" pH meter; the pH electrode was placed at the bottom of the plastic bucket used for purging. The discharge tubing was also placed at the bottom of the bucket being careful not to place it too near the pH electrode because a water current moving past the electrode can affect the pH reading. Once the bucket was filled and overflowing with water the pH was recorded.

One unfiltered sample, poisoned with about 100 μl of saturated $HgCl_2$ solution, was collected from each sampling location for the analysis of ^{13}C in DIC; also a second filtered but un-poisoned sample was collected for comparison from Well 11, Well 16, Salto Seep, and Guacimo Spring. The ^{13}C analyses were done in Neal Blair's carbon isotope lab, Dept. of Marine, Earth, and Atmospheric Sciences, NCSU (NCSU –MEAS). The samples were collected in 60 ml amber glass bottles with plastic, aluminum foil lined caps. The protocol used to collect these samples was developed from Spotl (2005), personal correspondence with George Burr at the University of Arizona –AMS Lab (Aug 2005), and personal correspondence with Neal Blair at NCSU-MEAS (Sept 2005). Approximately 10 inches of copper tubing, of the same diameter as the copper intake

tubing, was attached to the discharge end of the viton tubing to be used hereafter as the discharge tube. The copper discharge tube was placed on the bottom of the bottle and water was allowed to fill the vial and overflow at least 3 container volumes (180 ml), at which point the discharge tube was removed from the bottle. A small portion of the water (<1 ml) was poured out and 2 drops (about 100 µl) of saturated $HgCl_2$ solution was added (this step was skipped for those samples that weren't poisoned). The bottle was then closed tightly, wiped dry, and electrical tape was wrapped around the cap. Upon analysis it was determined that the integrity of these samples was lost, therefore their data was not used in this study.

One unfiltered sample poisoned with about 300 µl of saturated $HgCl_2$ solution was collected from each sampling location for the analysis of ^{14}C and $\delta^{13}C$; also a second non-poisoned sample was collected for comparison from Well 11, Well 16, and Guacimo Spring. These samples were analyzed at the NOSAMS lab at Woods Hole Oceanographic Institute (WHOI). The samples were collected in 500 ml glass bottles with a 29/26 standard taper ground glass joint and solid glass stopper (McNichol and Jones 2003). WHOI supplied these bottles. The samples were collected using a protocol provided by WHOI (McNichol and Jones 2003). The copper discharge tube was placed at the bottom of the bottle and at least 2 container volumes (1000 ml) of water were allowed to overflow out of the bottle. While one person was filling the bottle, another person was applying a thin layer of Apiezon-M grease to the stopper in a wavy pattern with a 10 ml syringe. Once the bottle was filled, about 5 ml of water was poured out of the bottle, and the inside of the neck of the bottle was wiped dry using a laboratory wipe (Kim-wipe) wrapped around a finger. 6 drops (about 300 µl) of saturated $HgCl_2$ solution

was added to preclude microbial activity (this step was skipped for those samples that weren't poisoned). The stopper was twisted into the bottle neck to ensure a good seal. The bottle was wiped dry and electrical tape was wrapped around the stopper and bottle from top to bottom.

Two unfiltered samples were collected from each of the sampling locations for the analysis of tritium (one tritium sample was taken from Well 20). The samples were collected in 500 ml narrow mouth LDPE bottles. This type of sample collection was recommended by the University Of Utah Dissolved Gas Laboratory. The cap was rinsed three times with water from the sampling site immediately before sample collection. The discharge tube was then placed at the bottom of the bottle and at least 2 container volumes (1000 ml) of water were allowed to overflow (at Well 11 and the Arboleda weir only 1 container volume was allowed to overflow), at which point the discharge tube was removed and the bottle was capped and wiped dry.

Two samples filtered to 0.70 μm using a glass fiber filter were acidified with 100 μl of 6N HCl for the analysis of S, NO_3^-, and DOC (all analyzed from the same sample). The samples were collected in 60 ml glass vials with silicon septa. The septa were not glued to the caps because glued septa may contaminate DOC samples (Guillermo Ramirez, NCSU-SS, 08/2005). The protocol used to collect these samples was developed from Standard Methods of Water and Wastewater Analysis (1998) and personal communication with Guillermo Ramirez NCSU-SS (08/2005). The discharge tube was placed on the bottom of the vial and water was allowed to fill the vial and overflow about 3 container volumes (180 ml), at which point the discharge tube was removed from the vial. A small portion (several drops) was poured out to allow space for the HCl. 2 drops

(about 100 µl) of 6N HCl was then added to the sample to preclude microbial activity. The vials were capped and wiped dry. Upon returning from the field to the lab at La Selva the samples were placed in a refrigerator.

Four unfiltered samples were collected for the analyses of CFCs (two CFC samples were taken at Arbo weir). Samples were collected in 125 ml glass bottles with aluminum foil lined screw-caps. This type of bottle and cap was recommended by the United State Geological Survey (USGS) CFC Laboratory in Reston, VA (http://water.usgs.gov/lab/chlorofluorocarbons/). The bottle and cap (foil liner facing down) were placed in the 1L plastic bucket used for purging. The discharge tube was placed at the bottom of the bottle. 2 liters of water for the first sample (1L for the remaining 3 samples) was allowed to flow through the bottle, keeping the bottle submerged once the bucket was filled. The cap was tapped underwater to dislodge any air bubbles. If no bubbles were present in the cap, it was screwed on the bottle, all while keeping both the bottle and cap completely submerged. Once the cap was on the bottle, the bottle was removed from the plastic bucket and turned upside down to see that there were no bubbles in the bottle. If no bubbles were present, the cap was tightened further and secured with at least two rounds of electrical tape applied in a clockwise direction. If air bubbles were present the process was repeated. The overflow water was left in the tub for the remaining samples. The bottles were wiped dry and upon returning to the lab at La Selva were stored upside down in a refrigerator.

Two samples were collected from each of the sampling locations (except Arbo weir and Taco weir where none were taken, and Well 20 and Well 30 where only one sample was taken) for the analysis of sulfur hexafluoride (SF_6). The samples were

collected in 1L safety coated glass bottles with polyseal cone lined screw-caps. This type of bottle and cap were recommended by the USGS CFC laboratory in Reston, VA (http://water.usgs.gov/lab/sf6/). The cap was rinsed three times with water from the sampling site immediately before collection. The discharge tube was placed at the bottom of the bottle. After the bottle was allowed to overflow at least two container volumes (2L) (at Well 20 only 1L was allowed to overflow), the discharge tube was removed. The cap was screwed on without headspace then secured with at least two rounds of electrical tap applied in a clockwise direction.

One sample filtered to 0.45 μm was collected from each sampling location for the precipitation of AgCl to be analyzed for ^{36}Cl. The samples were collected in 1 liter LDPE bottles. 1-4 liters of water was collected at each site depending on preliminary data on Cl concentration and the maximum rate at which each well could be pumped. Each bottle and cap was rinsed three times with filtered water from the site immediately before sample collection. Special care was taken not to touch the inside of the jug or cap. After the sample was taken and the lid was screwed on tightly the bottle was wiped dry. After returning to the lab at La Selva, AgCl was precipitated from the sample as described in the "Lab Methods" section.

Two samples were collected for the analysis of dissolved helium-3 (^3He) and other trace gases (Ne, Ar, Kr, N_2, O_2, CH_4, and various isotopes of Xe). The samples were collected in a 3/8" diameter, 30" long, copper tube that contained approximately 40 ml of water. This type of sample collection was recommended by the USGS CFC Laboratory and the University Of Utah Dissolved Gas Laboratory. A check valve was placed on one end of the copper tubing and the other was attached to the pump tubing.

The copper tubing was then lowered, check valve first, down the well. Using a hand vacuum pump, the copper tube was rinsed thoroughly by pumping water through it. Once rinsed and when no air bubbles could be seen in the tubing, the pump was reversed to pressurize the sample tube. The copper tube was then removed from the well and placed in an aluminum channel where the ends were clamped with metal pinch clamps to seal them.

4.2 Laboratory Methods

Water samples were analyzed using six different methods. ^{14}C and ^{13}C were analyzed by accelerator mass spectrometry (AMS) at Woods Hole Oceanographic Institution (WHOI). ^{36}Cl was analyzed by AMS by Prime Lab (Purdue rare isotope measurement laboratory) at Purdue University. ^{18}O was measured by isotope ratio mass spectrometry at the US Geological Survey Menlo Park Stable Isotope and Tritium Laboratory. Major ions (Ca^{2+}, K^{+}, Mg^{2+}, Na^{+}, Cl^{-}, SO_4^{2-}) and DOC were analyzed by ion chromatography and the combustion infrared method respectively at the Analytical Services Lab at the NCSU Department of Soil Sciences (NCSU-SS). Alkalinity was determined by titration in the lab at La Selva Biological Station. Except for ^{36}Cl, sample preparation was conducted in the field on the day of sampling following procedures described in Field Methods (4.1).

At WHOI ^{14}C and ^{13}C analysis began with converting DIC in the water samples to CO_2 which was then reacted with a catalyst to form graphite. The graphite was then pressed into a small cavity in an aluminum target. The surface of the graphite was sputtered with heated cesium, producing ions which were extracted and accelerated in the

AMS system (http://www.nosams.whoi.edu/clients/data.html). A mass spectrometer magnet with a 110º bending angle dispersed the C atoms into three isotope beams, ^{12}C, ^{13}C (encountering the most deflection), and ^{14}C (encountering the least amount of deflection) (http://www.nosams.whoi.edu/about/index.html). ^{13}C and ^{12}C were measured using Faraday Cups, ^{14}C was measured using a gas ionization counter (http://www.nosams.whoi.edu/clients/data.html). ^{13}C is expressed here as $\delta^{13}C$ (section 2.2). ^{14}C activities were reported by WHOI as Fraction Modern (F_m) which is a measurement of the deviation of the $^{14}C/^{12}C$ ratio of a sample from "modern" (F_m values were multiplied by 100 to give "percent modern carbon", pmC). Modern is defined as 95% of the radiocarbon concentration (in 1950) of NBS Oxalic Acid I normalized to $\delta^{13}C_{VPDB}$ = -19 per mil (Olsson, 1970). AMS results are calculated using the internationally accepted modern $^{14}C/^{12}C$ ratio of $1.176 \pm 0.010 \times 10^{-12}$ (Karlen et al. 1968). A final ^{13}C-correction is made to normalize the sample F_m to a $\delta^{13}C_{VPDB}$ value of -25 per mil (http://www.nosams.whoi.edu/clients/data.html). Average of the precision values (one standard deviation) reported by WHOI for the ^{14}C analyses in this study was about 0.6%; the average precision of the $\delta^{13}C$ analyses done at the WHOI AMS laboratory is 0.5‰ (McNichol 9/2006, pers. comm.).

In order for ^{36}Cl to be analyzed it had to first be precipitated from the water samples as AgCl. The procedure for the precipitation of AgCl was developed from personal communications with Dr. Thomas Torgersen at the University of Connecticut (7/05) and a series of lab experiments (Appendix 1). Within 12-15 hours of collection, each water sample taken for the analysis of ^{36}Cl was poured into a 1 gallon Rubbermaid tray in the laboratory at La Selva Biological Station. The pH of the water was measured

using pH test strips then HNO_3 was added to lower the pH below 3 in order to prevent interference from anions of weak acid such as CO_3^{-2} (Skoog and West 1980, pages 571-620). Aqueous 0.282 N $AgNO_3$ was then added to the sample until the concentration of Ag^+ in the mixture exceeded the concentration of Cl^-. The solution was allowed to sit for 2-5 days while the AgCl precipitate settled out onto the inner surface of the tray. After the settling period the water was poured out of the tray and a rubber policeman (blade of approximately 1cm) was used to scrape the AgCl precipitate from its inner surface into a pile. The precipitate was allowed to air dry in the lab at La Selva then collected using a plastic v-shaped spatula and kept in a brown 60 ml plastic bottle (precipitate from well 20, Salto seep, Well 30, and Saltito seep was dried in an oven at NCSU-MEAS at 65ºC for 24 hrs). AMS analysis of ^{36}Cl at Purdue was analogous to the analysis of ^{14}C. The AgCl precipitate was used as the target material from which atoms are sputtered by heated cesium (http://www.physics.purdue.edu/primelab/introduction/ams.html). ^{36}Cl concentrations in the AgCl are reported as a normalized radionuclide/stable nuclide ratio ($^{36}Cl/Cl$). This ratio is computed as $^{36}Cl/Cl = (^{36}Cl/^{37}Cl) \times 0.2423$. The constant 0.2423 is the natural abundance of ^{37}Cl (http://www.physics.purdue.edu/primelab/results/weburs_help.html). The range of precision values (one standard deviation) reported by Purdue for the $^{36}Cl/Cl$ analyses in this study was 11% to 150% (Appendix 1).

Mass spectrometry was used for analysis of ^{18}O. ^{18}O analyses were done at the USGS stable isotope lab in Menlo Park, CA. They were carried out by equilibrating each sample with CO_2 then analyzing the CO_2 with an isotope ratio mass spectrometer (Genereux 2004). Results are expressed as $\delta^{18}O$. $\delta^{18}O$ is the difference between the

$^{18}O/^{16}O$ of the sample and the $^{18}O/^{16}O$ of a standard, Vienna Standard Mean Ocean Water (VSMOW), in parts per thousand, ‰ (Coplen et al. 2000). Precision (one standard deviation) of $\delta^{18}O$ analyses at this laboratory is about 0.1‰.

Ion chromatography was used to determine the dissolved concentration of major cations (Ca^{2+}, K^{+}, Mg^{2+}, Na^{+}) and major anions (Cl^{-}, SO_4^{2-}). Anions and cations are measured separately but the principle behind each analysis is the same (Standard Methods 1998, Method 4110 B). A small sample (~5ml) was poured into a small plastic vial then the water was injected into the chromatograph in a stream of eluent (1mM $NaHCO_3$/8 mM Na_2CO_3 for anions, and 33 mM methanosulfonic acid for cations) and carried through a column packed with ion exchange resin (alkyl ammonium functional groups for anion exchange, sulfonic acid for cation exchange). Different ions were retained on the column for different lengths of time and were identified on this basis. The ion chromatograph was equipped with a conductivity detector. Precision (one standard deviation) of cation and anion analyses at this laboratory is about 6%.

The combustion infrared method was used to determine the concentration of dissolved organic carbon (DOC) (Standard Methods 1998, Method 5310 B). About 10ml of water was poured into the storage vessel on the carbon analyzer. A sample of water (25µl) was transferred from the storage vessel to a heated (650ºC) reaction chamber with aluminum oxide bullets covered with a platinum catalyst. The CO_2 produced from the oxidation of TDC was measured with a nondispersive infrared analyzer. (Standard Method 1998, Methods 5310 B) A second sample (25µl) was transferred from the storage vessel to a different reaction chamber filled with phosphoric acid to measure the DIC as the CO2 driven off from the sample after this acidification (some of the original DIC was

probably also lost by this same mechanism after the samples were acidified in the field). DOC was then determined from the difference between TDC and DIC (Standard Methods 1998, Method 5310 B). Precision (one standard deviation) of DOC analyses at this laboratory is about 6%

Alkalinity was determined using a Hach Alkalinity Single Parameter Test Kit with digital titrator (cat # 2063700). Each titration was done in the laboratory at La Selva Biological Station on the same day the sample was taken. The digital titrator is a digital burette with a titration cartridge containing H_2SO_4 and a delivery tube inserted into the titration cartridge. The manufacturer claims a precision of 0.02 mN for alkalinity titrations with this system. The titration was conducted with either a 1.6 N or 0.16 N H_2SO_4 cartridge, depending on the alkalinity expected based on previous data (Genereux et al. 2005), using a water sample mass of 100 g in an Erlenmeyer flask. A bromcresol green-methyl red indicator was added to each sample in the form of a Hach powder pillow (cat. # 23292-32). Following the instructions in the Hach method 8203, the sample was titrated to a pH of 5.1, 4.8, and then 4.5. The volume of H_2SO_4 required to reach each endpoint was recorded as the number on the digital counter of the titrator body. Each digit on the counter is equal to an H_2SO_4 addition of 0.00125 ml. The equation used to calculate the alkalinity of each water sample is

$$\left(\frac{acid_{(digits)} \times (0.00125 ml/digit) \times H_2SO_{4(eq/L)}}{mass_{(g)} / (0.997044 g/ml)} \right) \times \left(1000 meq/eq \right) = Alkalinity(meq/L)$$

where $acid_{(digits)}$ is the volume of H_2SO_4 added in digits, 0.00125*ml/digit* is the conversion factor to convert digits of H_2SO_4 to ml, $H_2SO_{4(eq/L)}$ is the concentration of acid H_2SO_4 used in the titration, $mass_{(g)}$ is the mass (in grams) of the water sample titrated, 0.997044*g/ml* is the density of water at 25ºC, and 1000*meq/eq* is the conversion factor to give Alkalinity in meq/L (mN). Uncertainty of this method is 0.02 mN with a titrant concentration of 1.6 N, and 0.002 mN with a titrant concentration of 0.16 N.

Chapter 5. Results and Discussion

5.1 Carbon

The waters at La Selva have a wide variation in carbon chemistry. Taconazo waters (wells 16, 7, 18, and Taco weir) and well 14 have low DIC, Cl^-, and $\delta^{13}C$, and high ^{14}C activity (Table 5.1). Wells 11, 13, and the Arbo weir in the lower Arboleda, well 20 and Salto seep in the Salto swamp have high DIC, Cl^-, and $\delta^{13}C$, and low ^{14}C activity (Table 5.1). Well 30 and Saltito seep in the Saltito swamp are intermediate in DIC, Cl^-, and $\delta^{13}C$, and high ^{14}C (Table 5.1).

Table 5.1. Chemical results from water sampling at and near La Selva Biological Station in March 2006 and upslope from La Selva in the possible recharge area on Volcan Barva in December 2006 (BCNP 1 only).

Sampling location	DIC mM	DOC mM	$\delta^{13}C$ of DIC ‰ VPDB	^{14}C of DIC pmC	Cl^- mM	$^{36}Cl/Cl$ multiply by 10^{-15}	$\delta^{18}O$ ‰ VSMOW	CFC-12 pcmole/ kg	CFC-113 pcmole/ kg
Well 11	8.77	<0.0833	-7.58	21.7	0.4620	24	-4.99	0.13761	0.01719
Well 13	5.22	0.133	-15.49	59.9	0.203	27	-4.53	1.03221	0.15792
Well 14	1.70	0.200	-25.54	112	0.0649	10	-4.35	1.71232	0.24720
Arbo weir	4.42	0.0749	-4.39	17.7	0.429	26	-4.33	1.02288	0.13870
Well 16	<1.49	<0.0833	-24.34	117	0.0508	112	-4.24	1.62109	0.24300
Well 7	<3.01	0.200	-26.00	117	0.0592	228	-4.35	1.66449	0.25722
Well 18	1.74	0.0833	-23.45	99.7	0.0592	7	-4.37	1.68979	0.24412
Taco weir	0.26	0.391	-22.35	109	0.0621	160	-3.07	1.56040	0.23946
Well 20	11.32	<0.0833	-6.80	18.0	0.666	17	-4.63	0.82901	0.10114
Salto Seep	11.68	<0.0833	-5.24	10.4	0.728	13	-4.79	0.16627	0.01608
Well 30	1.47	0.316	-20.20	83.4	0.0846	590	-4.17	1.44846	0.18732
Saltito seep	2.50	0.425	-5.83	29.7	0.299	69	-4.27	1.17202	0.15484
Guacimo spring	13.92	0.0833	-4.89	7.98	0.914	17	-4.26	0.07815	0.01188
BCNP 1	1.82	0.0441	-26.43	114					

In support of the conceptual hydrologic model we set out to test (page 2), an inverse correlation exists between Cl^- and ^{14}C. This correlation is of the form of $y= a/x + b$, which is consistent with a mixture of two waters with differing isotope chemistry

(Faure 1986, Ch. 9). ^{14}C vs. Cl^- can be modeled with the equation $^{14}C = 6.022/[Cl^-] + 9.141$, $r^2 = 0.9605$ (Figure 5.1). In this data set well 13 is the only significant outlier. This may be the result of acquisition of modern CO_2 by the groundwater during sampling; the water level at well 13 was at the top of the well screen before sampling, and dropped at least 4 cm during sampling. Thus, some groundwater reaching the well during sampling was likely running down the inside of the top of the screen. If well 13 is ignored the correlation is nearly identical: $^{14}C = 6.159/[Cl^-] + 6.146$, $r^2 = 0.9806$.

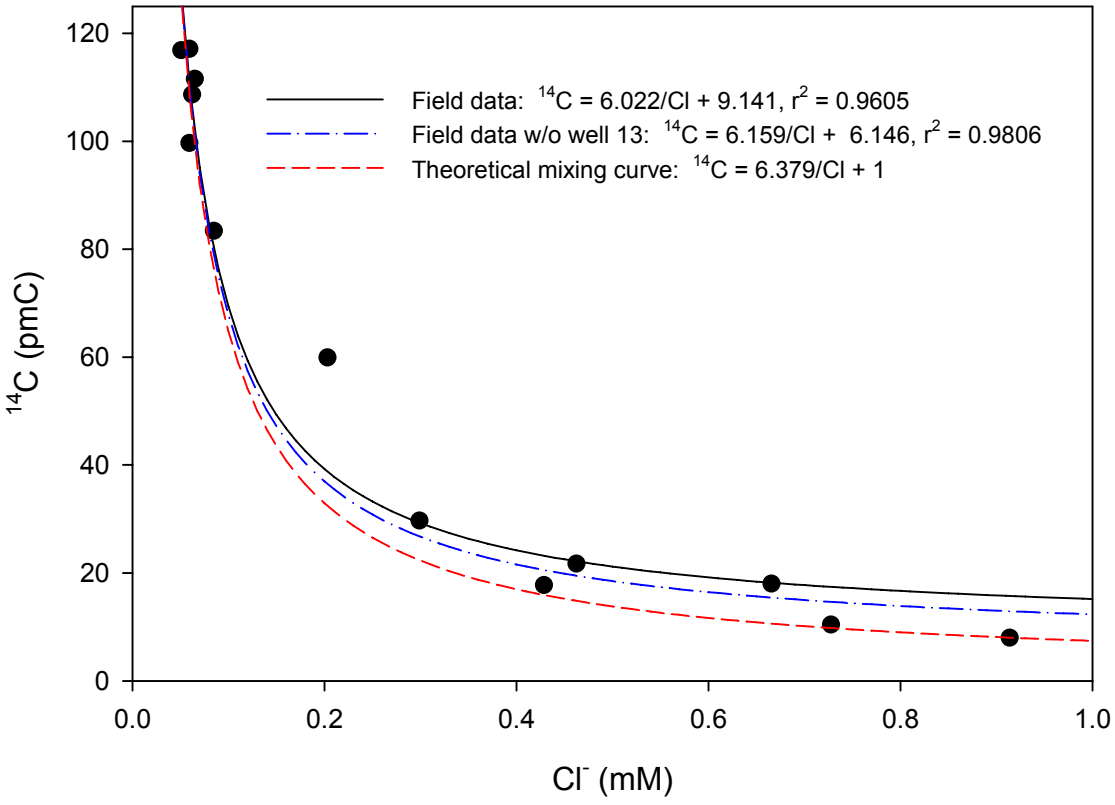

Figure 5.1. ^{14}C (in DIC) vs. Cl^-

Both correlations lie close to the relationship between a theoretical mixture of two distinct endmember waters: "bedrock groundwater" from Guacimo spring and "local water" represented by the average of low-solute high-^{14}C groundwater from wells 16 and 7: $^{14}C = 6.379/[Cl^-] + 1$ (see Figure 5.1). Finally, a similar correlation is present between $\delta^{13}C$ and Cl^-: $\delta^{13}C = -1.184/[Cl^-] - 4.440$, $r^2 = 0.9275$ (Figure 5.2). These results are not only consistent with the hypothesized mixing of two distinct groundwaters, but also the mixing of two waters that derive their DIC from two different sources of carbon.

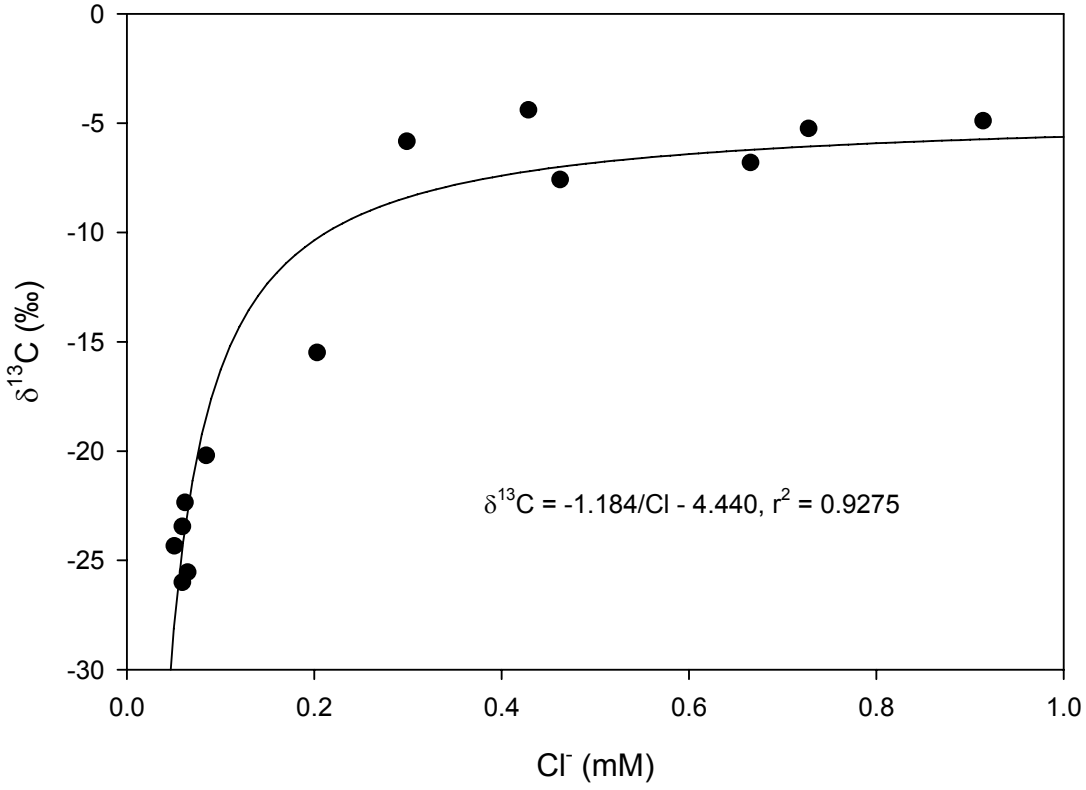

Figure 5.2. $\delta^{13}C$ (in DIC) vs. Cl^-

In an area with no carbonate rocks or minerals, the main source of carbon in recharging groundwater is from soil CO_2. The concentration of CO_2 in the soil zone is many times greater than that of the atmosphere due to microbial and plant root respiration (Kalin 2000). Galimov (1966) reported $\delta^{13}C$ in soil CO_2 to range from -21.1‰ to -28‰, the average being -24.7‰, which is similar to what other researchers have found (-23.3‰ by Cerling et al. 1991). Many groundwater studies have found -25‰ to be a reasonable value to use for the $\delta^{13}C$ of DIC derived from soil CO_2 (e.g., Pearson and White 1967; Fontes and Garnier 1979). This is consistent with the range of $\delta^{13}C$ of soil CO_2 found at La Selva (-21‰ to -26‰) (Schwendenmann 2001, 2002), and local groundwaters from the Taconazo watershed (wells 16, 7, 18) and well 14 in the Arboleda watershed (-22‰ to -26‰).

If low-solute groundwater from our lowland wells 7, 14, 16, and 18 (with average DIC = 1.42 mM and $\delta^{13}C$ = -24.8‰) is representative of recharge, upslope on Volcan Barva, to the bedrock groundwater system discharging at Guacimo spring (DIC = 13.92 mM and $\delta^{13}C$ = -4.89‰), then bedrock groundwater acquires about 12.50 mM of DIC high in ^{13}C between recharge and discharge. Sample BCNP 1 (DIC = 1.82 mM) might also serve well as a model for recharge to the bedrock groundwater system (^{18}O data in Genereux (2004) suggest bedrock groundwater recharge at roughly the elevation where BCNP 1 was collected), in which case the addition of DIC between recharge and discharge would be 12.1 mM. Magmatic CO_2 is a possible source for this DIC.

Williams-Jones et al. (2000) found evidence for diffuse magmatic degassing through the lower flanks of Volcan Arenal (75 km northwest of Barva), Volcan Poas (25 km northwest of Barva), and Galeras (Columbia). The effect of this was enriched $\delta^{13}C$ in

CO_2 and higher concentrations of Rn and CO_2 in soil gases on the lower flanks of these three volcanoes. In this work it is suggested that a majority of the CO_2 degassed through the flanks of these volcanoes is dissolved into the groundwaters of regional aquifers, carried downslope, and exsolved from the water upon discharge. This kind of transport of magmatic CO_2 by cold groundwaters has been documented in the North American Cascades (Evans et al. 2002; James et al. 1999; Rose et al. 1996), Italy (Chiodini et al. 2000; Allard et al. 1997), and Japan (Ohsawa et al. 2002). Carbon isotope and DIC concentration data presented here suggest that a similar scenario is present on Volcan Barva, where bedrock groundwater (as sampled at Guacimo Spring) acquires a significant amount of DIC by dissolution of magmatic CO_2 before reaching La Selva.

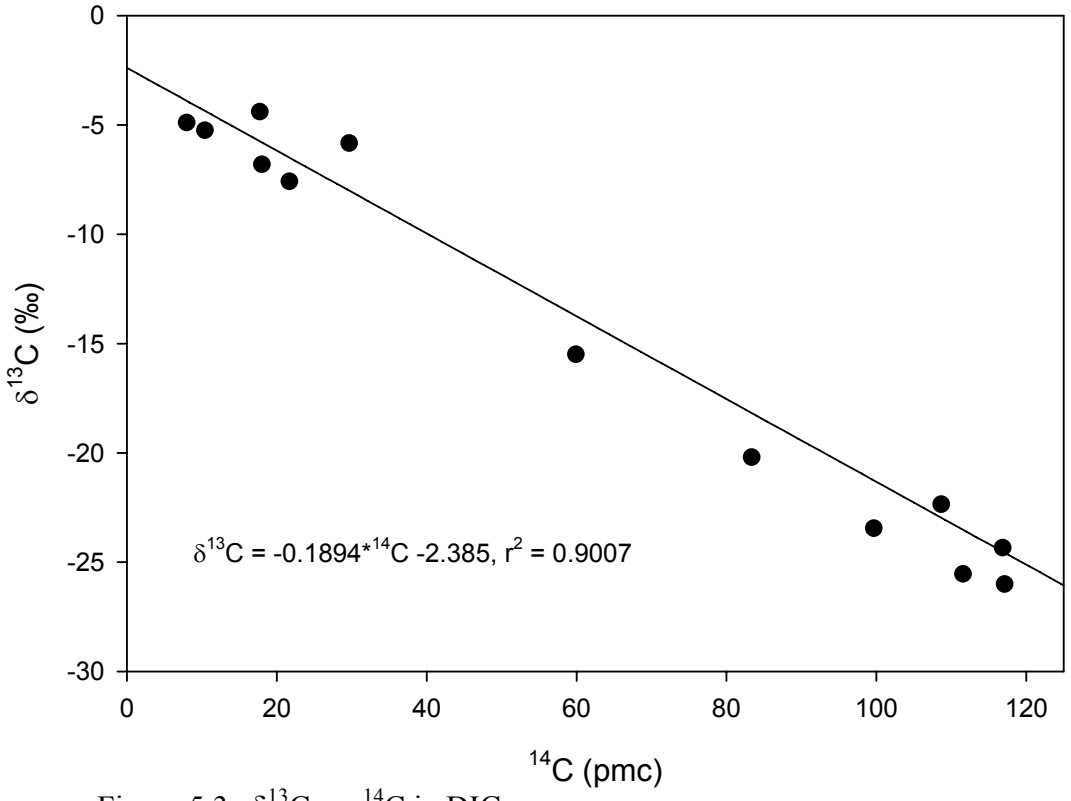

Figure 5.3. $\delta^{13}C$ vs. ^{14}C in DIC

When shown on a $\delta^{13}C$ vs. ^{14}C plot, the data from La Selva (Figure 5.3) fit very well on a mixing line consistent with two sources of DIC. A regression line through the data gives an indication of the carbon sources. The presence of bomb ^{14}C in low-solute groundwaters with $\delta^{13}C$ of about -25‰ indicates that the low-$\delta^{13}C$ carbon source is typical of modern soil CO_2. If the other C source is magmatic CO_2 (which would have ^{14}C = 0 pmc) Figure 5.3 suggests this source would have a $\delta^{13}C$ = -2.4±0.2‰. This is consistent with $\delta^{13}C$ values of -2.7±0.3‰ from CO_2 collected directly from Arenal magmas (Delorme et al. 1981) and $\delta^{13}C$ = -2.5 to -3.0‰ collected from fumaroles on Momotombo, Nicaragua (Allard 1980). These samples are considered to be representative of the bulk gas content of the melt because they have a low nitrogen gas content, N_2 = 1-3% and <1%, and were taken at high temperature, 810-950ºC and 749ºC, for Arenal and Momotombo respectively. N_2 is almost absent from igneous rocks and high-temperature volcanic gas, and high temperature gases (>750ºC) are considered less contaminated and more closely representative of the gas content of the magma (Allard 1983).

Although the $\delta^{13}C$ of mantle derived carbon is between -5 and -8‰ (Javoy et al. 1986; DesMarais and Moore 1984), CO_2 from subduction zone volcanoes is known to vary from -2.7‰ at Volcan Arenal to -11.5‰ at Mount St. Helens (Javoy et al. 1986). Javoy et al. (1986) proposed two possibilities for the high $\delta^{13}C$ and the variations in $\delta^{13}C$ of CO_2 outgassed from subduction zone volcanoes. First, in certain cases on continental margins magmas rise through variable thicknesses of continental crust that may contain sedimentary carbonate. If the magma is undersaturated with respect to carbon, it can dissolve a certain amount of sedimentary carbon. The enrichment in $\delta^{13}C$ would

correspond to the amount of incorporated carbonate. Second, if derived from deep in the mantle wedge, ascending magmas outgas to various degrees until they reach the base of the crust. An isotope fractionation effect of 3 to 4.5‰ associated with exsolution of CO_2 gas from magma has been documented by Javoy et al. (1978), Des Marais and Moore (1984), and Pineau and Javoy (1986). Therefore the first CO_2 exsolved from a magma at $\delta^{13}C$ = -7‰ will have a $\delta^{13}C$ of -2.5 to -4.0‰. If magmas stop at higher levels they will become more outgassed and more depleted. Also, Poorter et al. (1991) and Sumino et al. (2004) suggested that the composition of volcanic gases may be influenced by subducted oceanic crust (including carbonate sedimentary formations) in the Sunda and Banda arcs in Indonesia ($\delta^{13}C$ for CO_2 of -3‰) and the Izu-Ogasawara arc in Japan ($\delta^{13}C$ for CO_2 of 1.5‰) respectively.

In general, low ^{14}C and elevated DIC and Ca concentrations may be indications that groundwater has interacted with carbonate rocks in the subsurface. However, information on the physical geological environment and the water chemistry at Guacimo Spring suggest that interaction with carbonate rocks does not account for the low ^{14}C and elevated DIC and Ca concentrations at this spring.

The study site sits near the boundary between two geological provinces (Limon marine sedimentary basin and the volcanic province that includes the Cordillera Central). It is not certain what the deep geology is beneath La Selva (there are no deep boreholes at the site, only a water supply well drilled to about 50 m showing all volcanic rocks), but the recharge area for IGF discharging at La Selva is obviously in the volcanic Cordillera (the only area of high elevation adjacent to La Selva). It seems likely that IGF flowpaths originating there would predominantly interact with the geology of that province even if

La Selva itself sits on the western edge of Limon Basin deposits. Working with the incomplete but best available information on Costa Rica geology, the depth to the shallowest limestone beneath the Cordillera Central is roughly 1700 m beneath the Quaternary volcanics that comprise Volcan Barva (Weyl 1980) (depth to the shallowest limestone in the Limon Basin is at least 5750 m, although the clastic formations above that, possibly starting at a depth of 50 m, are known to have localized intercalations of limestone; Weyl 1980). It seems unlikely that IGF flowpaths discharging at La Selva would have penetrated 1700 m into the crust between the recharge and discharge areas. Groundwater flow on the south side of Volcan Barva is concentrated through the lava flows oriented roughly parallel to the general topography of Barva; these fractured lavas represent high permeability horizons between much lower-permeability ignimbrites (Parker et al. 1988). If the same can be inferred on the north side of Barva (the side upslope from La Selva) it would suggest that groundwater involved in IGF into La Selva does not circulate deeply enough to contact limestone beneath the Cordillera. Still, the geological information on the study site is not so precise as to rule out, on its own, the possibility that: (1) La Selva sits over the western edge of Limon Basin deposits, and (2) IGF flowpaths originating in the Cordillera pass through some Limon Basin carbonate materials before discharging at La Selva.

However, chemical and isotopic data from our best sampling site for bedrock groundwater involved in IGF (Guacimo Spring) are atypical of deep groundwater having significant interaction with carbonate rocks. At Guacimo Spring DIC (13.92 mM) is higher while Ca and pH (0.78 mM and 6.13 respectively) are lower than what is generally found in groundwater in carbonate rocks (<5 mM, 1-3 mM , and 7-9 for DIC, Ca, and pH

respectively; Freeze and Cheery 1979, page 263; Plummer and Sprinkle 2001; McIntosh and Walter 2006). These data are more consistent with the source of carbon being CO_2 rather than solid carbonate.

Finally, Figure 5.3 suggests that the source of elevated DIC in IGF to La Selva has a $\delta^{13}C$ value (-2.4 ± 0.2‰) somewhat lower than that of marine carbonate rocks (such as those in the Limon Basin) and closer to that of magmatic CO_2 in subduction zones. The $\delta^{13}C$ values of marine carbonate rocks of Cambrian to Tertiary age fall in a very narrow range around zero (Faure 1986, pages 497-498). Keith and Weber (1964) obtained an average $\delta^{13}C$ value of 0.56 ± 1.55‰ for 321 samples of marine carbonate rocks.

For reasons discussed above, it is unlikely that interaction with carbonate rocks is the cause of elevated DIC and low ^{14}C activity of the water being discharged at Guacimo Spring. The available evidence is more consistent with these effects being caused by addition of magmatic CO_2 with a $\delta^{13}C$ of about -2.4 and ^{14}C activity of 0 pmc (figure 5.3 and related discussion).

Two factors may therefore contribute to the low ^{14}C activity of water discharging from Guacimo Spring: radioactive decay and addition of magmatic CO_2 without ^{14}C. Because CFCs have been detected in the water discharged at Guacimo Spring (although at concentrations near the lower limit of detection, see Table 5.1), the ^{14}C activity of this water may have been increased slightly by a small amount of young water mixing in with the older bedrock groundwater at the spring. All these effects must be distinguished in order to isolate the effect of radioactive decay on ^{14}C activity and estimate the age of the bedrock groundwater. NETPATH a geochemical mass-balance modeling program

(Plummer et al. 1994), was used to account for inputs of magmatic CO_2 and mixing with younger water to estimate the age of the bedrock groundwater. NETPATH simulations often focus on chemical weathering in groundwater and associated mass transfers between groundwater and aquifer solids. Because there are likely no carbon bearing solids (carbonate minerals or solid sedimentary organic matter) in these volcanic rock aquifers, some very simple simulations were used, with only one geochemical mass transfer into the groundwater (input of magmatic CO_2), a few geochemical reactions involving C in the groundwater (carbonate equilibria and oxidation of DOC), and mixing with a young local water.

Using NETPATH to model geochemical changes along a flowpath in the bedrock groundwater system required defining an "initial water", a “mixing water”, and a "final water" so that mass transfers could be calculated along the flowpath between the initial and final water (initial water + mass transfers + mixing = final water). The final water was the water discharged at Guacimo Spring, and the water to be dated was the bedrock groundwater portion of the final water. The measured chemistry of water from Guacimo Spring (temperature, density, pH, dissolved O_2, specific conductance, major ion concentrations, DOC and DIC concentrations, $\delta^{13}C$, and ^{14}C) was entered into NETPATH to define the final water in all simulations. The only parameters necessary to define for magmatic CO_2 were its $\delta^{13}C$ and ^{14}C activity of -2.4‰ (Figure 5.3) and 0 pmc (all carbon in the magmatic system was assumed to be >50,000 years old), respectively (inputs for NETPATH are summarized in Table 5.2).

Table 5.2. Input data significant to NETPATH models, see text for details.
A: Average of concentrations in young local water at wells 7, 14, 16, and 18.
B: Simulations were run with values of -26, -25, -24, and -22 (see text).
C: Simulations were run with values of -26, -25, and -24 (equal to the $\delta^{13}C$ of biogenic CO_2 in initial water).
D: Assumed (see text)
E: Calculated using equation 5.1
F: Simulations were run with CFC-12 or CFC-113, not both in the same simulation.
G: Measured in sample BCNP 1 from Volcan Barva.
H: Equal to the $\delta^{13}C$ of biogenic CO_2 (-24, -25, or -26) under Approach 1, or -26.43 under Approach 2.
I: Simulations were run with different values for DOC from different sources

	Initial water Approach 1	Initial water Approach 2	Young water	Final water	Magmatic CO_2
DIC (mM)	1.42[A]	1.82[G]	1.42[A]	13.92	NA
DOC (mM)	0.13[A]	0.13[A]	0.13[A]	0.08	NA
TDC (mM)	1.55	1.95	1.55	14.00	NA
$\delta^{13}C$ DIC (‰)	-22 to -26[B]	-26.43[G]	H	-4.89	-2.4
$\delta^{13}C$ DOC (‰)	-25[D]	-25[D]	-25[D]	-25[D]	NA
^{14}C DIC (pmc)	91.5-100[E]	100[D]	111.3[A]	7.93	0
^{14}C DOC (pmc)	100[D]	100[D]	111.3[D]	0, 50, 100[I]	NA
CFC-12[F]	0	0	1.672[A]	0.07815	NA
CFC-113[F]	0	0	0.2479[A]	0.01188	NA

The initial water was a model, as it always is in ^{14}C groundwater dating studies (a sample of the recharge water that actually evolved into the final water is of course never available). The model for the initial water may be a modern sample from the recharge area, if this area is known and if the sample is free of "bomb ^{14}C"; even this best-case scenario involves the assumption that the physical location of the recharge area and the chemistry of the groundwater there have not changed significantly from the time of recharge of the final water to the present. When shallow groundwater samples free of bomb ^{14}C can not be found in the recharge area, the carbon isotope chemistry of the

initial water in a NETPATH simulation is generally based on one of the mass-balance carbon models in the literature (e.g., Eichinger 1983; Fontes and Garnier 1979).

Two different approaches were used to define the initial water in NETPATH simulations aimed at estimating the age of bedrock groundwater (Table 5.2):

Approach 1: carbon in the initial water was viewed as biogenic CO_2, with or without a small component of magmatic CO_2, and with DIC and DOC concentrations and $\delta^{13}C$ of DIC constrained by our data from lowland wells at La Selva.

Approach 2: data from BCNP 1, collected from a groundwater seepage point on a hillside at about 660 m elevation in the possible recharge area for bedrock groundwater, were used to define the concentration and $\delta^{13}C$ of DIC, while DOC concentration was defined as in Approach 1.

In Approach 1, NETPATH simulations were run in which the initial water had DIC = 1.42 mM (average of low-solute local water at wells 7, 14, 16, and 18), ^{14}C = 100 pmc (a common assumption in ^{14}C dating studies concerning pre-bomb biogenic CO_2, when there is no solid calcite in soil in the recharge area), and $\delta^{13}C$ = -24, -25, or -26‰ (based on the mean of $\delta^{13}C$ of -24.8 at wells 7, 14, 16, and 18). These models assume a bedrock groundwater recharge area upslope from La Selva, toward Volcan Barva, in which the shallow groundwater is unaffected by magmatic CO_2 and is thus similar to shallow local groundwater at La Selva. Simulations were also run in which the initial water was defined as having biogenic CO_2 (above) with varying amounts (<20%, Table 5.2) of magmatic CO_2. Studies on the Arenal, Poas, and Galeras volcanoes found magmatic CO_2 in soil gas ($\delta^{13}C$ in soil gas ranged from -12 to -26‰; Williams-Jones 2000), suggesting its presence in shallow groundwater as well. In order to investigate the

possible effects of this on groundwater age estimates, simulations were run in which CO_2 of soil gas had $\delta^{13}C$ = -24‰ (soil CO_2 being a mixture of magmatic CO_2 having a $\delta^{13}C$ = -2.4‰ and biogenic CO_2 having a $\delta^{13}C$ = -25 or -26‰) or -22‰ (soil CO_2 being a mixture of magmatic CO_2 and biogenic CO_2 having a $\delta^{13}C$ = -24‰, -25‰, or -26‰). DIC in these simulations was held at the same value (1.42 mM) used for simulations in which there was no magmatic CO_2 in the initial water. While it's reasonable to suppose the presence of magmatic CO_2 in the unsaturated soil zone might increase the DIC of shallow groundwater, there is evidence that soil pCO_2 is only very weakly correlated (if at all) with $\delta^{13}C$ of soil gas on other volcanoes (Figure 5.4), suggesting that addition of magmatic CO_2 does not necessarily increase soil pCO_2 (and thus might not increase DIC of shallow groundwater).

For those simulations in which the initial water was modeled using Approach 1 where the DIC of the initial water was a mixture of magmatic CO_2 (with ^{14}C=0 pmc) and biogenic CO_2 (with ^{14}C=100 pmc), the ^{14}C activity of the initial water ($^{14}C_i$) was calculated as $^{14}C_i$ (pmc) = $100F_b$, where F_b is the fraction of DIC derived from biogenic CO_2. F_b from a simple mixing equation:

$$F_b = \frac{\delta^{13}C_i - \delta^{13}C_m}{\delta^{13}C_b - \delta^{13}C_m} \qquad \text{(Eq. 5.1)}$$

where $\delta^{13}C_i$ is $\delta^{13}C$ of DIC in the initial water, $\delta^{13}C_m$ is the $\delta^{13}C$ of the magmatic CO_2 (-2.4‰), and $\delta^{13}C_b$ is $\delta^{13}C$ of biogenic CO_2 (-24, -25, or -26‰).

Under Approach 2 to defining the initial water in NETPATH simulations, the concentration and $\delta^{13}C$ of DIC in initial water were defined based on the values measured in groundwater sample BCNP 1 (Table 5.1) taken upslope from La Selva on the flanks of Volcan Barva at an elevation of about 660 m (in the possible recharge area for bedrock

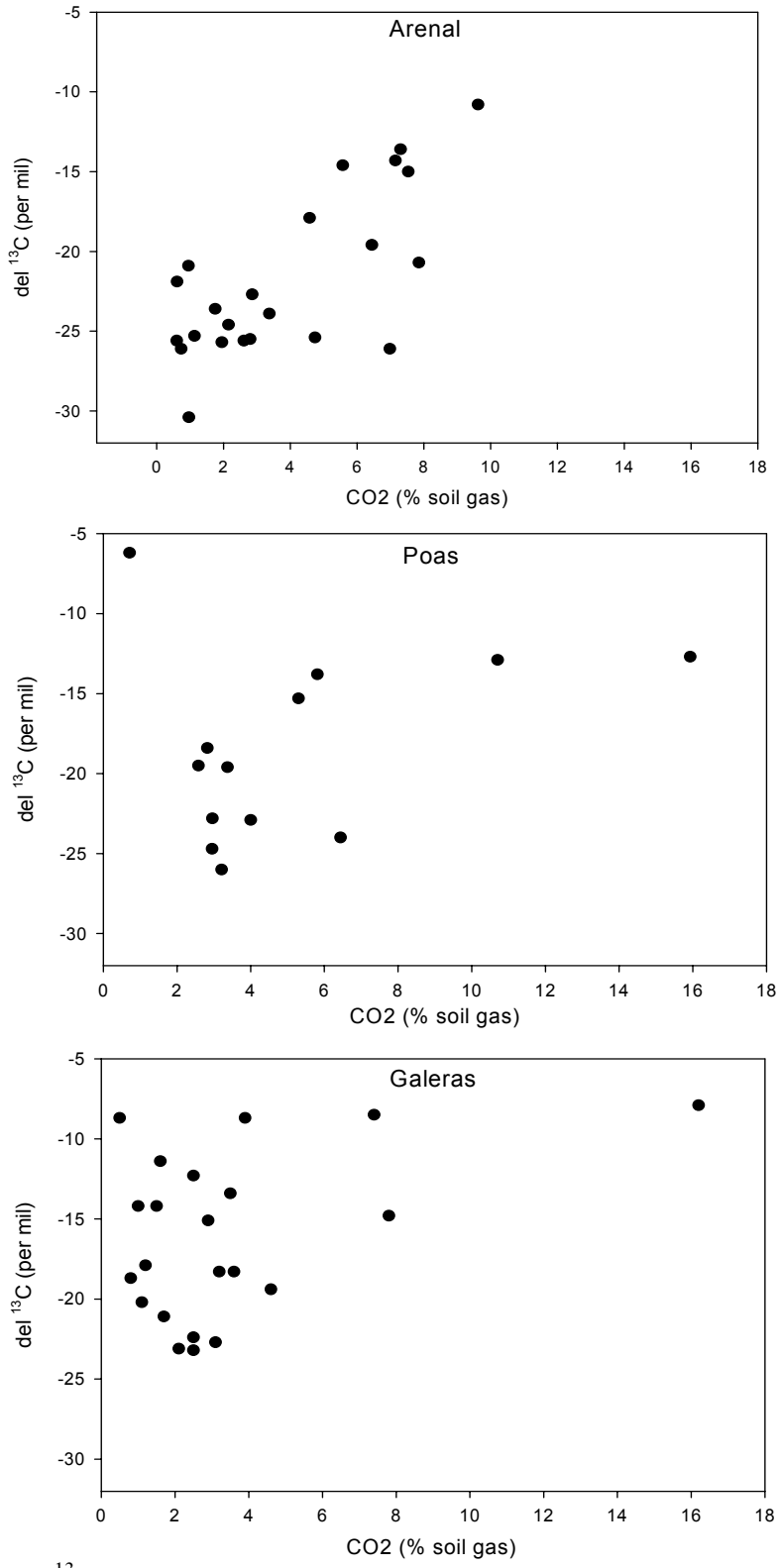

Figure 5.4. $\delta^{13}C$ vs CO_2 from soil gas on Arenal, Poas, and Galeras. Data from Williams-Jones et al. (2000).

groundwater). The low $\delta^{13}C$ of this sample suggests that magmatic CO_2 is not present in the shallow groundwater at this site.

The small amount of young local water that mixes with bedrock groundwater at Guacimo Spring (as indicated by the non-zero CFC concentrations in the spring water) was modeled in a manner analogous to the initial water (without magmatic CO_2) under Approach 1: its chemical and isotopic characteristics were defined as averages of the measured values at the low-solute local water wells 7, 14, 16, and 18 (Table 5.2). In all the NETPATH simulations, the $\delta^{13}C$ of DIC in this young local water was taken as equal to the $\delta^{13}C$ of biogenic CO_2 in the initial water. Two separate sets of simulations were run, one using CFC-12 as the constraint on young water mixing and the other using CFC-113 as the constraint; each of these CFCs suggests that just under 5% of the Guacimo spring discharge is due to young local water.

Finally, a $\delta^{13}C$ and ^{14}C activity of DOC must also be assigned to each of the waters described above. $\delta^{13}C$ of DOC was assumed to be -25‰. This is a common assumption in groundwater dating studies (Geyh 2000; Plummer et al. 1990; Plummer and Sprinkle 2001), and within the range found in studies of isotopic compositions of DOC in groundwater, -24‰ to -31‰ (Wassenaar et al. 1990; Aravena and Wassenaar 1993). Because this aquifer is composed of volcanic formations, having little if any organic carbon, DOC is most probably derived from decomposition of soil organic matter in the recharge area. Therefore, ^{14}C activity of DOC for the initial water and the young, local water were set at 100 pmc and 111.3 pmc respectively. ^{14}C activity of DOC in the final water was initially set at 0 pmc (Table 5.3), but because at least some portion (if not all) of DOC in the final water was acquired from the recharge area (accounted for in the

initial water) or from mixing with young local water, simulations were also done in which the ^{14}C activity of DOC in the final water was set at 50 pmc and 100 pmc where mixing was constrained only by CFC-12.

The results of the NETPATH simulations are in Table 5.3 and 5.4. The only simulations presented from Approach 1 are those in which the difference between $\delta^{13}C$ computed for the final water and $\delta^{13}C$ observed at Guacimo Spring (used as a check on the simulation) was less than 0.5‰ (the approximate analytical precision for the $\delta^{13}C$ analyses). The simulations that fell within this range all had $\delta^{13}C_i$ = -26 to -22‰, suggesting little or no influence of magmatic CO_2 on the initial water. The simulations in which initial water was modeled under Approach 2 had slightly larger differences between computed and observed $\delta^{13}C$ of 0.6‰ to 0.8‰. The addition of 5% local modern water had little effect on the $^{14}C_{nd}$ (^{14}C activity of bedrock groundwater in the absence of radioactive decay calculated by NETPATH) of Guacimo Spring and the calculation of the age of the bedrock groundwater. 5% local modern water with DIC = 1.42 mM accounts for only about 0.5% of the carbon in the final water at Guacimo Spring, allowing for very little effect. While this small mixing with young local water at Guacimo Spring had very little effect on calculated age, it is more accurate to include it than to not do so.

Where ^{14}C activity of DOC in the final water was 0 pmc, the simulations using Approach 1 yielded $^{14}C_{nd}$ values of 9.34 pmc to 11.12 pmc, which together with the measured ^{14}C activity at Guacimo Spring (7.93 pmc) lead to ^{14}C ages of about 1400 to 2800 years before present. The simulations modeling the initial water with Approach 2 yielded $^{14}C_{nd}$ values of 13.83 to 13.92 pmc, resulting in ^{14}C ages of 4600 to 4650 years

before present. Increasing the ^{14}C activity of DOC in the final water adds ^{14}C to the bedrock groundwater, this decreases the difference between $^{14}C_{nd}$ and ^{14}C of the final water, lowering its age. Therefore the simulations in which ^{14}C activity of DOC in the final water was 100pmc had the lower ages (750-2200 yrs form Approach 1 and 3640 yrs for Approach 2; Table 5.4). All of these ages seem plausible for travel through a regional groundwater system. Stable isotopic evidence ($\delta^{18}O$ in water) suggests that bedrock groundwater discharging at Guacimo Spring is recharged at an elevation of about 700 m (Genereux 2004), which occurs on Volcan Barva at a distance of about 15 km from Guacimo Spring, in an area that receives about 8 m of rain annually. This distance and the estimated ages of groundwater suggest average linear velocities on the order of 3-20 m/yr in the bedrock groundwater system, high at the upper end but possible, depending on the exact values of recharge rate, porosity, and cross-sectional area of the aquifer. Most likely age values are probably those based on Approach 2 to the initial water (i.e. those giving the largest ages and smallest groundwater velocities).

Table 5.3. NETPATH simulation results for Guacimo Spring. "$\delta^{13}C_{bio}$" is the $\delta^{13}C$ of biogenic CO_2 in the initial water and in the young water which mixes into Guacimo Spring near the spring. "$\delta^{13}C_i$" is the $\delta^{13}C$ of DIC in the initial water (which differs from $\delta^{13}C_{bio}$ in simulations in that there is some magmatic CO_2 in the initial water). "$^{14}C_i$" is the ^{14}C activity of the initial water, "%BGW in GS" is the percent bedrock groundwater in Guacimo Spring water (based on CFC concentrations, or set to 100 for the simulations with no mixing of young local water), "$\delta^{13}C$ TDC" is the $\delta^{13}C$ of TDC (total dissolved carbon), "$\delta^{13}C$ (DIC)" is the $\delta^{13}C$ of DIC, "$^{14}C_{nd}$" is the ^{14}C activity of the final water in the absence of ^{14}C decay (used with the measured ^{14}C activity at Guacimo Spring to calculate the age of the bedrock groundwater), and "^{14}C" is the ^{14}C activity measured at Guacimo Spring. The simulations using Approach 2 to model the initial water are those with $\delta^{13}C_i = \delta^{13}C_{bio} = -26.43‰$; all others were based on Approach 1.

Input				Results							
mixing				% BGW	$\delta^{13}C$ (total)		$\delta^{13}C$ (DIC)		$^{14}C_{nd}$	^{14}C	age
constraint	$\delta^{13}C_{bio}$	$\delta^{13}C_i$	$^{14}C_i$	in GS	computed	observed	computed	observed	computed	observed	years
none	-26	-26	100.0	100.00	-5.0013	-5.009	-4.8821	-4.89	11.0622	7.9337	2748
none	-26	-24	91.5	100.00	-4.7988	-5.009	-4.6783	-4.89	10.1220	7.9337	2014
none	-26	-22	83.1	100.00	-4.5962	-5.009	-4.4745	-4.89	9.1927	7.9337	1218
none	-25	-25	100.0	100.00	-4.9001	-5.009	-4.7802	-4.89	11.0622	7.9337	2748
none	-25	-24	95.6	100.00	-4.7988	-5.009	-4.6783	-4.89	10.5755	7.9337	2376
none	-25	-22	86.7	100.00	-4.5962	-5.009	-4.4745	-4.89	9.5909	7.9337	1568
none	-24	-24	100.0	100.00	-4.7988	-5.009	-4.6783	-4.89	11.0622	7.9337	2748
none	-24	-22	90.6	100.00	-4.5962	-5.009	-4.4745	-4.89	10.0223	7.9337	1932
none	-26.43	-26.43	100.0	100.00	-5.7306	-5.009	-5.6157	-4.89	13.9157	7.9337	4645
CFC-12	-26	-26	100.0	95.32	-5.0014	-5.009	-4.8821	-4.89	11.1208	7.9337	2792
CFC-12	-26	-24	91.5	95.32	-4.8083	-5.009	-4.6879	-4.89	10.2245	7.9337	2097
CFC-12	-26	-22	83.1	95.32	-4.6152	-5.009	-4.4936	-4.89	9.3387	7.9337	1348
CFC-12	-25	-25	100.0	95.32	-4.9001	-5.009	-4.7802	-4.89	11.1208	7.9337	2792
CFC-12	-25	-24	95.6	95.32	-4.8035	-5.009	-4.6831	-4.89	10.6568	7.9337	2439
CFC-12	-25	-22	86.7	95.32	-4.6104	-5.009	-4.4889	-4.89	9.7183	7.9337	1677
CFC-12	-24	-24	100.0	95.32	-4.7988	-5.009	-4.6783	-4.89	11.1208	7.9337	2792
CFC-12	-24	-22	90.7	95.32	-4.6057	-5.009	-4.4841	-4.89	10.1296	7.9337	2020
CFC-12	-26.43	-26.43	100.0	95.32	-5.6985	-5.009	-5.5834	-4.89	13.8407	7.9337	4600
CFC-113	-26	-26	100.0	95.20	-5.0014	-5.009	-4.8821	-4.89	11.1208	7.9337	2793
CFC-113	-26	-24	91.5	95.20	-4.8085	-5.009	-4.6881	-4.89	10.2271	7.9337	2099
CFC-113	-26	-22	83.1	95.20	-4.6157	-5.009	-4.4941	-4.89	9.3425	7.9337	1351
CFC-113	-25	-25	100.0	95.20	-4.9001	-5.009	-4.7802	-4.89	11.1223	7.9337	2793
CFC-113	-25	-24	95.6	95.20	-4.8036	-5.009	-4.6832	-4.89	10.6589	7.9337	2441
CFC-113	-25	-22	86.7	95.20	-4.6108	-5.009	-4.4892	-4.89	9.7216	7.9337	1680
CFC-113	-24	-24	100.0	95.20	-4.7988	-5.009	-4.6783	-4.89	11.1223	7.9337	2793
CFC-113	-24	-22	90.6	95.20	-4.6050	-5.009	-4.4843	-4.89	10.1323	7.9337	2022
CFC-113	-26.43	-26.43	100	95.20	-5.6977	-5.009	-5.6977	-4.89	13.8338	7.9337	4599

Table 5.4 NETPATH simulation results for Guacimo Spring with ^{14}C of DOC at Guacimo Spring (^{14}C of DOC_f) equal to 50 pmc (top 9 simulations) and 100 pmc (lower 9 simulations). All other notation is consistent with Table 5.3. Mixing is constrained by CFC-12 (percent bedrock groundwater in Guacimo Spring water is 95.32).

Input			Results								
			^{14}C of	$\delta^{13}C$ (total)		$\delta^{13}C$ (DIC)		$^{14}C_{nd}$	^{14}C	age
$\delta^{13}C_{bio}$	$\delta^{13}C_i$	$^{14}C_i$	DOC_f	computed	observed	computed	observed	computed	observed	years
-26	-26	100.0	50	-5.0000	-5.009	-4.8807	-4.89	11.1146	8.2300	2484
-26	-24	91.5	50	-4.8069	-5.009	-4.6865	-4.89	10.2188	8.2300	1789
-26	-22	83.1	50	-4.6138	-5.009	-4.4922	-4.89	9.3336	8.2300	1040
-25	-25	100.0	50	-4.8987	-5.009	-4.7788	-4.89	11.1146	8.2300	2484
-25	-24	95.6	50	-4.8021	-5.009	-4.6817	-4.89	10.6509	8.2300	2132
-25	-22	86.7	50	-4.6091	-5.009	-4.4875	-4.89	9.7130	8.2300	1370
-24	-24	100.0	50	-4.7974	-5.009	-4.6770	-4.89	11.1146	8.2300	2484
-24	-22	90.7	50	-4.6043	-5.009	-4.4827	-4.89	10.1345	8.2300	1721
-26.43	-26.43	100.0	50	-5.5775	-5.009	-5.4617	-4.89	13.2505	8.2300	3937
-26	-26	100.0	100	-5.0000	-5.009	-4.8807	-4.89	11.1146	8.5264	2191
-26	-24	91.5	100	-4.8069	-5.009	-4.6865	-4.89	10.2188	8.5264	1497
-26	-22	83.1	100	-4.6138	-5.009	-4.4922	-4.89	9.3336	8.5264	748
-25	-25	100.0	100	-4.8987	-5.009	-4.7788	-4.89	11.1146	8.5264	2191
-25	-24	95.6	100	-4.8021	-5.009	-4.6817	-4.89	10.6509	8.5264	1839
-25	-22	86.7	100	-4.0910	-5.009	-4.4875	-4.89	9.7130	8.5264	1077
-24	-24	100.0	100	-4.7974	-5.009	-4.6770	-4.89	11.1146	8.5264	2191
-24	-22	90.6	100	-4.6043	-5.009	-4.4827	-4.89	10.1240	8.5260	1420
-26.43	-26.43	100	100	-5.5775	-5.009	-5.4617	-4.89	13.2505	8.5264	3644

5.2 Chloride

Like the carbon data, there is a broad range of Cl concentrations and $^{36}Cl/Cl$ ratios. When a regression model of the form y = a/x + b is applied to the $^{36}Cl/Cl$ and Cl data (as was done for ^{14}C vs. Cl), the resulting correlation is weak, $^{36}Cl/Cl \times 10^{-15} = 7.7391/[Cl]+32.4079$, $r^2 = 0.1240$ (Figure 5.5). The data support the mixing of two waters, one with low Cl concentration and a highly variable $^{36}Cl/Cl$ ratio, and the other with a high Cl concentration and a lower and more consistent $^{36}Cl/Cl$ ratio (Figure 5.5, Table 5.4).

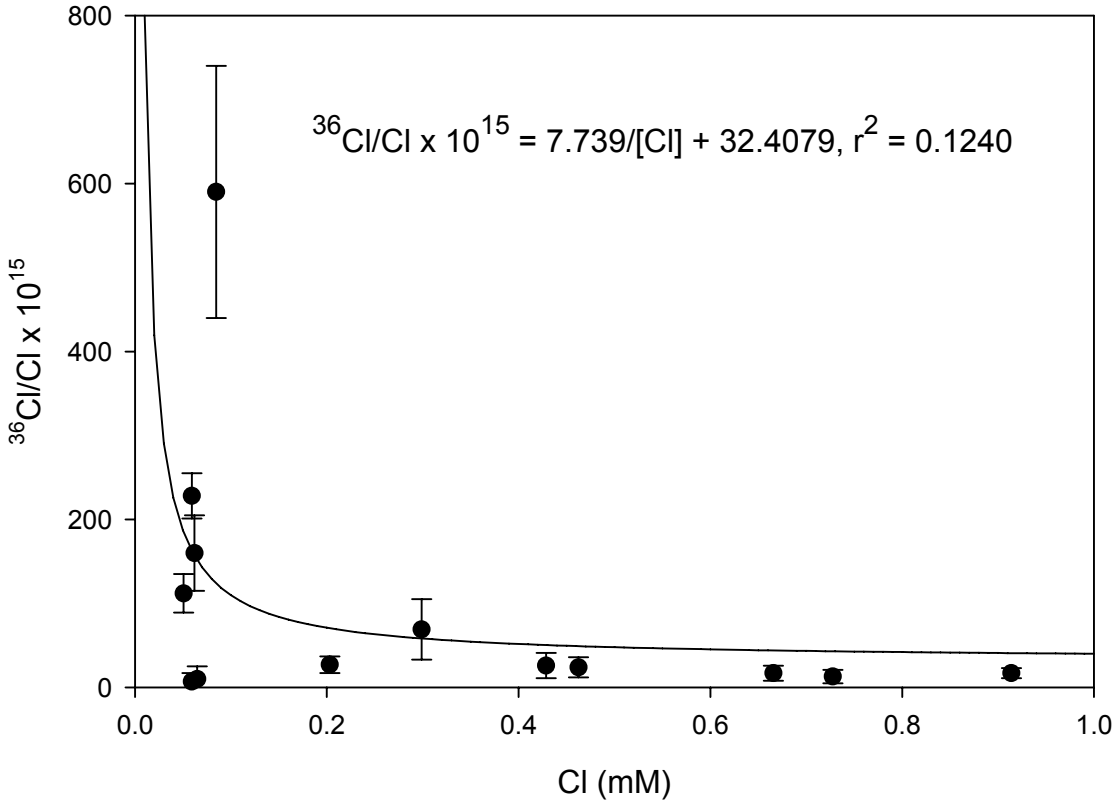

Figure 5.5. $^{36}Cl/Cl$ vs. Cl concentration. Error bars represent 1 standard deviation.

Table 5.5. Cl concentration and $^{36}Cl/Cl$ ratios, arranged from lowest to highest Cl concentrations.

Sampling location	Cl (mM)	$^{36}Cl/Cl$ Multiply value by 10^{-15}	Error in $^{36}Cl/Cl$ 1 std. dev.
Well 16	0.0508	112	23
Well 7	0.0592	228	27
Well 18	0.0592	7	10
Taco weir	0.0621	160	45
Well 14	0.0649	10	15
Well 30	0.0846	590	150
Well 13	0.2031	27	10
Saltito seep	0.2990	69	36
Arbo weir	0.4287	26	15
Well 11	0.4626	24	12
Well 20	0.6657	17	9
Salto Seep	0.7277	13	8
Guacimo spring	0.9139	17	6
BCNP 1	0.0550	130	75

Taken as whole, the Cl isotope and concentration data support the conceptual hydrologic model. Waters from well 30, the Taconazo watershed (wells 7, 16, 18, and Taco weir) and at higher elevation in the Arboleda watershed (well 14) contain atmospheric Cl, having a highly variable $^{36}Cl/Cl$ ratio, which is expected for water from a shallow local groundwater system not having the opportunity to acquire Cl with a more consistent $^{36}Cl/Cl$ ratio through the dissolution of subsurface volcanic rocks, or the time for dispersion to even out the short-term variability in the $^{36}Cl/Cl$ ratio of recharge. Data from Guacimo Spring are consistent with rainwater that has moved through mafic to andesitic volcanic rock and acquired significant dissolved Cl (with a lower and more consistent $^{36}Cl/Cl$) by dissolution of the volcanic host rocks and/or acquisition of Cl from interaction with magmatic fluids. Waters from the lower Arboleda watershed (wells 11, 13, and Arbo weir), the Salto swamp (well 20 and Salto seep), and Saltito seep appear to

be the result of bedrock groundwater (Guacimo spring) mixing with young local groundwater.

The low Cl waters (well 7, well 14, well 16, well 18, well 30, and Taco weir, having Cl from 0.0508 to 0.0846 mM) display a large variability in the $^{36}Cl/Cl$ ratio, 7 to 590 x 10^{-15}. This spatial variability in $^{36}Cl/Cl$ of local groundwater may ultimately be due to temporal variability in the $^{36}Cl/Cl$ of rainfall, for a local groundwater system, with no subsurface sources of Cl, in which the Cl is derived completely from atmospheric deposition. Seasonal fluctuations of ½ - 2 orders of magnitude in $^{36}Cl/Cl$ ratios have been documented in Greenland ice cores (Suter et al. 1987) as well as fluctuations of 2-3 orders of magnitude between precipitation events and/or monthly precipitation samples (Hainsworth et al. 1994; Knies et al. 1994; and Santos et al. 2004).

In Santos et al. (2004) and Hainsworth et al. (1994) low $^{36}Cl/Cl$ ratios were attributed to transport of "dead" marine-chloride (having a very low $^{36}Cl/Cl$ ratio) in the atmosphere from the Atlantic Ocean and Chesapeake Bay respectively, resulting in low $^{36}Cl/Cl$ ratios of Cl in precipitation. A similar situation exists at La Selva where marine Cl in precipitation was found to be concentrated during the dry season and diluted 50 to 100 fold during the wet-season (Eklund et al. 1997). Seasonal patterns in the chemical composition of precipitation (including Cl) became particularly significant during extreme conditions, such as during severe dry periods (Eklund et al. 1997).

Data collected at La Selva also show a correlation between H^+ and non-marine Cl and SO_4, as well as high concentrations of non-marine SO_4 in rainfall, with winds from the southwest (winds are normally out of the northeast) suggesting that, in addition to seasonal patterns described above, the frequent exhalation of volcanic gases from Volcan

Poas also influences the chemistry of precipitation at La Selva (Eklund et al. 1997). This is similar to what has been observed in tropical forests adjacent to active volcanism in Columbia (Veneklaas 1990). Genereux et al. (2005) found an additional atmospheric input of Cl in a hydrologic watershed budget study for the Arboleda and Taconazo watersheds from December 2000 to November 2001 consistent with additional Cl arising from acidic volcanic emissions on Volcan Poas during that time. Such an addition of Cl to the atmosphere would be expected to have a $^{36}Cl/Cl$ ratio of 5×10^{-15} to 15×10^{-15} (Rao et al. 1996; Hurwitz et al. 2005) similar to the $^{36}Cl/Cl$ ratio of well 14 and 18, which have recharge dates of 2000 to 2006 for different tracers (paper in prep by Skidmore, Genereux, Solomon and Plummer).

High $^{36}Cl/Cl$ ratios in non-marine, atmospheric Cl, comparable to that seen at well 30 (590×10^{-15}), are known to result from seasonal variations in stratosphere-troposphere mixing (Suter et al. 1987; Knies et al. 1994; Hainsworth et al. 1994). Air exchange across the tropopause between the stratosphere (where most ^{36}Cl is formed and $^{36}Cl/Cl$ is therefore high) and the troposphere is believed to be dominated by global processes such as large-scale meridional circulation and the associated shift in the Intertropical Convergence Zone (Keywood et al. 1998), which is the proposed reason for the seasonal variations in the $^{36}Cl/Cl$ of Greenland ice (Suter et al. 1987). Smaller scale processes associated with thunder storms that penetrate the lower stratosphere can also result in the collection and deposition of large amounts of ^{36}Cl in a specific area (Keywood et al. 1998; Santos et al. 2004).

Whatever the source, the fact that variability of an equal or lesser magnitude to that found in precipitation by Hainsworth et al. (1994), Knies et al. (1994), and Santos et

al. (2004) is found among the groundwater samples from this study is suggestive of a smaller, unconfined groundwater system where residence times are short enough to prevent dispersion in the groundwater from homogenizing or attenuating the short time scale variability in $^{36}Cl/Cl$ of recharge. This is also consistent with the range of CFC recharge dates for these waters; 1989 for the modern fraction of well 30, to 2001-2006 for well 14 (Skidmore 2007).

Waters from well 11, well 13, well 20, Salto seep, Saltito seep, Arboleda weir, and Guacimo Spring (previously described as having a significant fraction of deep bedrock groundwater) have much greater Cl concentrations (0.2031 mM to 0.9139 mM) than the waters discussed above. In these waters, concentration of atmospheric Cl in rain water through evaporation can be ruled out as a source of Cl. Evapotranspiration, having been estimated at 2 m in this area (Genereux et al. 2005), is no more than half of the rainfall at La Selva and less than that for up-gradient areas on the flanks of Volcan Barva (the proposed recharge area for the deep bedrock groundwater). This would result in a maximum increase in Cl concentration by a factor of about 2, but the high Cl waters are 4.5 to 18 times more concentrated than the low Cl waters described above.

The most notable difference between the low chloride and high chloride waters (>0.2 mM Cl), beside the Cl concentration, is the consistently low $^{36}Cl/Cl$ ratio of the high Cl waters. The highest-Cl water, at Guacimo Spring, may have been formed by rain water recharging the regional volcanic aquifer, on the flanks of Volcan Barva, with a small amount of atmospheric Cl and a highly variable $^{36}Cl/Cl$ ratio (resembling the low Cl local waters discussed above), and in the process of flowing from recharge to discharge, acquiring many times more Cl (of a lower and more consistent $^{36}Cl/Cl$)

through dissolution of the host rock and /or possible addition from magmatic fluid. Cl concentration and isotope data from the sites of intermediate Cl concentration (wells 11, 13, and 20, Saltito seep, Salto seep, and Arbo weir) are consistent with mixing between high-Cl, low-^{36}Cl/Cl bedrock groundwater and low-Cl, variable-^{36}Cl/Cl young local water.

Phillips (2000) found the average secular equilibrium ^{36}Cl/Cl ratios (background level) to be 25 x 10^{-15} (ranging from 7 to 34) in granites, and 7 x 10^{-15} (ranging from 3 to 15) in basalts. The andesites and basalts of Barva's lava flows would be expected to have a secular equilibrium ^{36}Cl/Cl ratio toward the low-to-middle part of this overall range. This would also be expected of any water moving through these formations for a significant amount of time, acquiring Cl through their dissolution. With a ^{36}Cl/Cl ratio of 17 x 10^{-15}, water from Guacimo Spring, which we view as the bedrock groundwater endmember in the conceptual mixing model, falls well within this range.

Because of the connection between the regional groundwater system and volcanic processes associated with Volcan Barva, specifically magmatic degassing (see section 5.1), Cl addition through the interaction with magmatic fluids also seems possible. Experimental data from Carroll and Webster (1994) suggest that halogens are incompatible in magmas, and readily partition into H_2O-rich phases. Cl condensed out of high-temperature fumaroles has been found to have ^{36}Cl/Cl ratios less than 15 x 10^{-15} (Rao et al. 1996). In the central Oregon Cascades; Hurwitz et al. (2005) concluded that high Cl concentrations in groundwaters were found to be the result of magmatic degassing (they felt that the observed Cl concentrations could not be accounted for by only Cl from weathering of rocks and relict formation waters from the sedimentary

rocks). These waters had $^{36}Cl/Cl$ ratios from 7 to 12 x 10^{-15} (Hurwitz et al. 2005). The waters that were the subject of this study are relatively dilute with respect to Cl, less than 0.91 mM compared to 27.45 mM in Hurwitz et al. (2005), but a similar $^{36}Cl/Cl$ ratio and the already demonstrated interaction with volcanic processes (section 5.1) suggest the addition of Cl from magmatic fluids as a possibility for deep bedrock groundwater.

5.3 Oxygen-18

In this study, no clear correlation between Cl and $\delta^{18}O$ presents itself amongst the data (Figure 5.6). When a linear regression model is applied the result is a weak correlation: $\delta^{18}O = -3.9852 - 0.8120[Cl]$, [Cl] in mM, $r^2 = 0.1980$.

The data from this study, based on March 2006 samples from 13 sites in and around La Selva, fall within the same range as data in Genereux (2004), based on 196 samples collected from March-July 2000 from 14 sites in and around La Selva. High variability among the lowest Cl samples is consistent with the view of these waters as young groundwater of different ages resulting from recharge of local precipitation with a highly variable isotopic signature (e.g., Genereux (2004) found the standard deviation of $\delta^{18}O$ in integrated weekly precipitation samples was 2.04‰); CFC and SF_6 recharge dates for these waters are 1988-2000. Less variability of higher Cl waters is consistent with the view of these waters as mixtures of temporally variable local groundwater with less variable bedrock groundwater.

The fact that the Guacimo Spring $\delta^{18}O$ data from this study falls more than 1 standard deviation (Figure 5.6) from the mean $\delta^{18}O$ found by Genereux (2004) could be due in part to the fact that there appears to be about 5% local water mixed with bedrock

groundwater at this site (see section 5.1), offering the possibility of temporal variability of $\delta^{18}O$ at Guacimo Spring. The difference between the $\delta^{18}O$ of Guacimo Spring from this study and the average $\delta^{18}O$ from Genereux (2004), as well as the temporal variability observed in Genereux (2004), are probably in part a reflection of this (as well as the measurement uncertainty, about ±0.2‰ at 95% confidence).

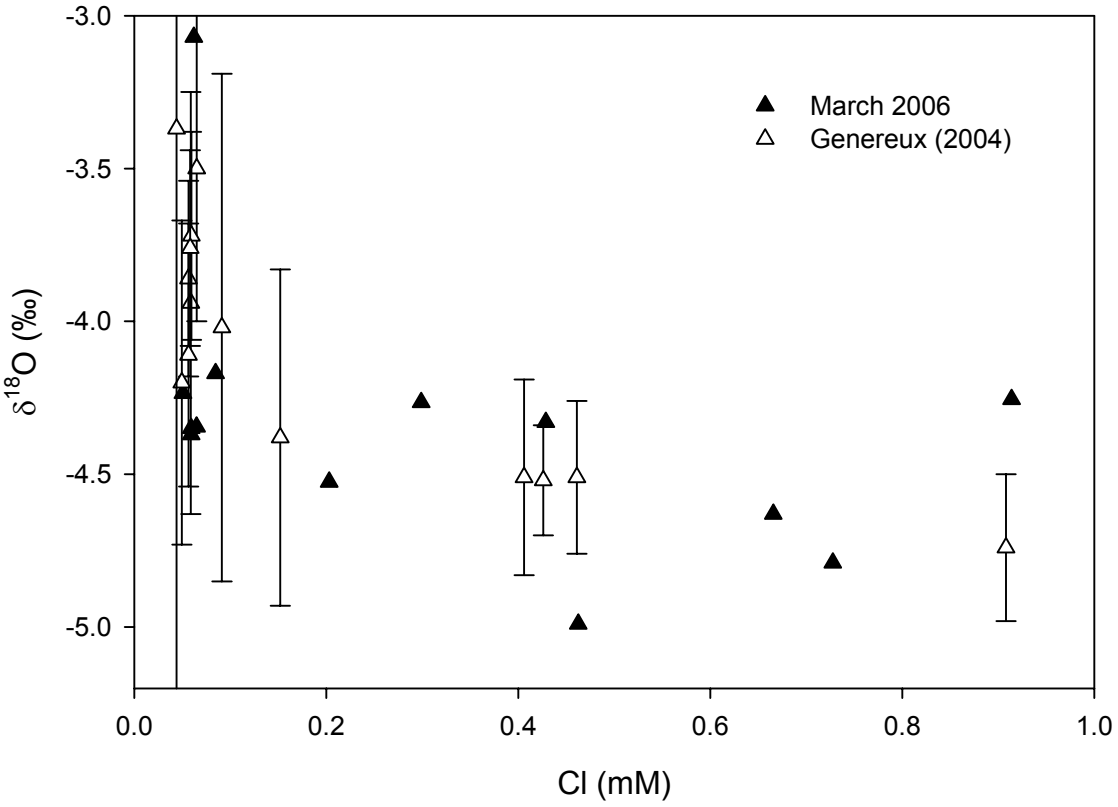

Figure 5.6. $\delta^{18}O$ vs. Cl data from March 2006 plotted with data from Genereux (2004). The error bars represent 1 standard deviation.

Chapter 6. Conclusion

The correlation between ^{14}C and Cl, and the correlation between $\delta^{13}C$ and Cl provide strong support for mixing between two endmember waters: a low-solute local water and a high solute bedrock groundwater (Guacimo Spring). Thus the carbon isotope data are consistent with the two component conceptual mixing model involving IGF.

The local water endmember has low DIC, a $\delta^{13}C$ of -24‰ to -26‰, $^{14}C > 100$ pmc (indicating relatively young groundwater containing "bomb" carbon), low Cl concentration, and a highly variable $^{36}Cl/Cl$ ratio (being derived from atmospheric deposition). The recharge dates for these waters were calculated as being between 1990 and 2000 from CFC and SF_6 data (Skidmore 2007). The bedrock groundwater endmember has a DIC of about 14 mM, a $\delta^{13}C$ of -3‰ to -5‰, $^{14}C < 8$ pmc (probably reflecting DIC from magmatic degassing of CO_2 on/near Volcan Barva's lower flanks), high Cl concentration and, a low and consistent $^{36}Cl/Cl$ ratio (consistent with Cl acquired through dissolution of the mafic and andesitic rocks that compose the aquifer and/or interaction with magmatic fluids).

NETPATH geochemical modeling of the chemical and isotopic data from the Guacimo spring discharge water constrains the likely recharge date of the bedrock groundwater to be between about 750 and 4600 years before present. These ages suggest average linear velocities of 3-20 m/yr in the bedrock groundwater system discharging into La Selva. The different ages and groundwater velocities result from different models of the concentration, $\delta^{13}C$, and ^{14}C of the DIC in recharge to the bedrock groundwater system (the "initial water" in NETPATH simulations) as well as variation in the assumed value of ^{14}C of DOC at Guacimo Spring. The larger ages (2800-4600 years) and smaller

groundwater velocities (3-5 m/yr) are probably more likely; they are based on initial water with DIC and $\delta^{13}C$ either constrained by data from a sample from the likely recharge area (Approach 2 in Section 5.1) or modeled without any influence of magmatic CO_2 in the shallow recharge (the simulations with Approach 1 giving the oldest ages).

With respect to the mixed waters, as the Cl concentration increases (indicating an increased concentration of bedrock groundwater), ^{14}C decreases, $\delta^{13}C$ increases, and the $^{36}Cl/Cl$ ratio decreases and becomes less variable. This is consistent with the deep bedrock groundwater described above discharging upward into the lowland watersheds at La Selva and mixing with the local groundwater. Results from the $\delta^{18}O$ data are consistent with previous work (Genereux 2004).

The conclusions from the carbon and chloride isotope data in this study are consistent with previous work which used major ion, ^{18}O, and physical hydrologic data. This suggests the conclusions about IGF and mixing of two distinct groundwaters at La Selva are robust and correct. Results also strongly suggest that IGF of bedrock groundwater is responsible for a large carbon flux into the lowland watersheds at La Selva, approximately 740 g of C per m^2 annually for the Arboleda watershed, based on multiplying the DIC concentration from Guacimo Spring by the average annual IGF of deep bedrock groundwater into the Arboleda watershed from 1998 to 2002 from Genereux et al. (2005) (4.40 m of bedrock groundwater IGF times 14 mM DIC, with appropriate units conversions to gC/m^2yr). This is significant when compared to a net ecosystem CO_2 exchange with the atmosphere of 0 to -800 g of C per m^2 annually (Loescher et al. 2003) and a CO_2 production/loss from the soil of 1200-1300 g of C per m^2 annually (Schwendenmann and Veldkamp 2006). This flux connects deep carbon

from tectonic and magmatic activity in the region to modern carbon cycling in the lowland rainforest. Future work may involve further quantifying and comparing the magmatically derived and non-magmatic DIC discharging from the rainforest watersheds at La Selva. Further study and quantification of diffuse degassing and dissolution of magmatic CO_2 into regional aquifers might also help constrain both weathering and magmatic intrusion rates near Volcan Barva and improve understanding of global inorganic carbon emissions.

References Cited and Bibliography

Allard, P., 1980. Composition isotopique du carbone dans les gaz d'un volcan d'arc: le Momotombo (Nicaragua). C.R. Academy of Science, Paris, 290: 1525-1528.

Allard, P. 1983. The origin of hydrogen, carbon, sulphur, nitrogen, and rare gases in volcanic exhalations: evidence from isotope geochemistry. Chapter 25 in: Forcasting Volcanic Events, Elsevier Science Publishers, New York, 635 pages.

Allard, P., P. Jean-Baptiste, W. D'Allessandro, F. Parello, B. Parisi, C. Flehoc. 1997. Mantle-derived helium and carbon in groundwaters and gases of Mount Etna, Italy. *Earth and Planetary Science Letters* 148: 501-516.

Alvarado-Induni, G.E. 1990. Caracteristicas geologicas de la Estacion Biologica La Selva, Costa Rica. *Tecnologica en marcha* 10(3): 11-22.

Aravena, R. L.I. Wassenaar. 1993. Dissolved organic carbon and methane in a regional confined aquifer, southern Ontario, Canada: Carbon isotopic evidence for associated subsurface sources. *Applied Geochemistry* 8: 483-493.

Aravena, R., L.I. Wassenaar, L.N. Plummer. 1995. Estimation of C-14 groundwater ages in a methanogenic aquifer. *Water Resources Research* 31(9): 2307-2317.

Atkinson, M. 1998. Selecting peristaltic pump tubing. *Machine Design* 70(4): 218-219.

Bentley, H.W., F.M. Phillips, S.N. Davis. 1986a. Chlorine-36 in the terrestrial environment. Chapter 10 in: P. Fritz, J.Ch. Fontes (eds), Handbook of Environmental Isotope Geochemistry, Volume 2: The Terrestrial Environment, Elsevier, New York, 544 pages

Bentley, H.W., F.M. Phillips, S.N. Davis, M.A. Habermehl, P.L.Airey, G.E. Calf, D. Elmore, H.E. Gove, T. Torgersen. 1986b. Chlorine 36 dating of very old groundwater 1. The Great Artesian Basin, Australia. Water Resources Research 22(13): 1991-2001.

Broecker, W.S., E.A. Olson. 1960. Radiocarbon from nuclear tests. *Science* 132: 712-721.

Carroll M.R., J.D. Webster. 1994. Solubilities of sulfur, noble gases, nitrogen, chlorine, and fluorine in magmas. *Review in Mineralogy: Volatile in magmas* 30: 231-274.

Castillo M, R. 1969. Geologicas de los mapas basicos abra y partes de Rio Grande, Costa Rica. Informes Tecnicos y Notas Geologicas. No. 33. San Jose:Minesterio de Industria y Comercio.

Cerling, T.E., D.K. Solomon, J. Quade, J.R. Bowman. 1991. On the isotopic composition of carbon in soil carbon dioxide. *Geochimica et Cosmochimica Acta* 55: 3403-3405.

Chiodini, G., F. Frondini. C. Cardellini. F. Parello, L. Peruzzi. 2000. Rate of diffuse carbon dioxide earth degassing estimated from carbon balance of regional aquifers: The case of central Apennine, Italy. *Journal of Geophysical Research* 105(B4): 8423-8434.

Coplen, T.B., A.L. Herczeg, C. Barnes. 2000. Isotope engineering-Using stable isotopes of the water molecule to solve practical problems. Chapter 3 In: P. Cook and A. Herczeg (eds.), Environmental Tracers in Subsurface Hydrology, Kluwer Academic Publishers, Boston, 529pages.

Craig, H. Geochemistry of stable carbon isotopes. 1953. *Geochimica et Cosmochimica Acta* 3: 53-92.

Deines, P. 1980. The isotopic composition of reduced organic carbon. Pages 329-406 in: P.Fritz, J.Ch. Fontes (eds), Handbook of Environmental Isotope Geochemistry, I. The Terrestrial Environment. Elsevier, Amsterdam.

Delorme, H., M. Javoy, J.L. Cheminee, F. Pineau. 1981. Chemical and isotopic compositions of volcanic gases from island arc and continental margins. Proceedings, 1st meeting of the European Union of Geosciences, Strasburg. *Terra Cognita*, Special Issue 1: 79 (abstract).

Desmarais, D.J., J.G. Moore. 1984. Carbon and its isotopes in mid-oceanic basaltic glasses. *Earth and Planetary Science Letters* 69: 43-57.

Eichinger, L. 1983. A contribution to the interpretation of ^{14}C groundwater ages considering the example of a partially confined sandstone aquifer. *Radiocarbon* 25: 347-356.

Eklund, T.J., W.H. McDowell, C.M. Pringle. 1997. Seasonal variation of tropical precipitation: La Selva, Costa Rica. *Atmospheric Environment* 31(22): 3903-3910.

Evans, W.C., M.L. Sorey, A.C. Cook, B.M. Kennedy, D.L. Shuster, E.M. Colvard, L.D. White, M.A. Huebner. 2002. Tracing and quantifying magmatic carbon discharge in cold groundwaters: lessons learned from Mammoth Mountain, USA. *Journal of Volcanology and Geothermal Research* 114: 291-312.

Faure, G. 1986. Isotope systematics of two-component mixtures. Chapter 9 in: Principles of Isotope Geology. John Wiley and Sons, New York, 589 pages.

Faure, G. 1986. Carbon. Chapter 26 in: Principles of Isotope Geology. John Wiley and Sons, New York. 589 pages.

Fehn, U., E.K. Peters, S. Tullai-Fitzpatrick, P.W. Kubik, P. Sharma, R.T.D. Teng, H.E. Grove, D. Elmore. 1992. ^{129}I and ^{36}Cl concentrations in waters of the eastern Clear Lake area, California: Residence times and source ages of hyrdrothermal fluids. *Geochimica et Cosmochimica Acta* 59: 2069-2079.

Fontes, J.C., J.M. Garnier. 1979. Determination of initial ^{14}C activity of the total dissolved carbon: A review of existing models and a new approach. *Water Resources Research* 5(2): 399-413.

Foster, S.S.D., A.T. Ellis, M. Losilla-Penon, and H.V. Rodriguez-Estrada. 1985. Role of volcanic tuffs in groundwater regime of Valle Central, Costa Rica. *Groundwater* 23(6): 795-801.

Francey, R.J., C.E. Allison, D.M. Etheridge, C.M. Trudinger, I.G. Enting, M. Leuenberger, R.L. Langenfelds, E. Michel, I.P. Steele. A 1000-year high precision record of $\delta^{13}C$ in atmospheric CO_2. 1999 *Tellus* 51B: 170-193.

Freeze, R.A., J.A. Cherry. 1979. Chemical evolution of natural groundwater. Chapter 7 in: Groundwater. Prentic Hall, New York, 604 pages.

Friedli, H., H. Lotscher, H. Oeschger, U. Siegenthaler, B. Stauffer. 1986. Ice core record of the $^{13}C/^{12}C$ ratio of atmospheric CO_2 in the past two centuries. *Nature* 324: 237-238.

Galimov, E.M. 1966. Carbon isotopes of soil CO_2. *Geochemistry International* 3: 889-897.

Genereux, D., C.M. Pringle. 1997. Chemical mixing model of streamflow generation at La Selva Biological Station, Costa Rica. *Journal of Hydrology* 199: 319-330. DOI 10.1016/SOO22-1694(96)03333-1

Genereux, D., S.J. Wood, C.M. Pringle. 2002. Chemical tracing of interbasin groundwater transfer in the lowland rainforest of Costa Rica. *Journal of Hydrology* 258: 163-178. DOI 10.1016/S0022-1694(01)00568-6

Genereux, D. 2004. Comparison of naturally-occuring chloride and oxygen-18 as tracers of interbasin groundwater transfer in lowland rainforest, Costa Rica. *Journal of Hydrology* 295: 17-27. DOI 10.1016/j.jhydrol.2004.02.020

Genereux, D.P., M.T. Jordan, D. Carbonell. 2005. A paired-watershed budget study to quantify interbasin groundwater flow in a lowland rain forest, Costa Rica. *Water Resources Research* 41: WO4011, DOI 10.1029/2004WR003635.

Geyh, M.A., H. Schleicher. 1990. Absolute Age Determination: Physical and Chemical Dating Methods and Their Application. Springer-Verlag, New York, 503 pages.

Geyh, M.A. 2000. An overview of ^{14}C analysis in the study of groundwater. *Radiocarbon* 42(1): 99-114.

Hainsworth, L.J., A.C. Mignerey, G.R. Helz. 1994. Modern chlorine-36 deposition in southern Maryland, U.S.A. *Nuclear Instruments and Methods in Physics Research* 92: 345-349.

Hartshorn, G.S., B.E. Hammel. 1994. Vegetation types and floristic patterns. Chapter 6 In: McDade, L.A., Bawa, K.S., Hespenheide, H.A., Hartshorn, G.S. (eds), La Selva: Ecology and Natural History of a Neotropical Rainforest, The University of Chicago Press, Chicago, 486 pages.

Hurwitz, S., R.H. Mariner, U. Fehn, G.T. Snyder. 2005. Systematics of halogen elements and their radioisotopes in thermal springs of the Cascade Range, Central Oregon, Western USA. *Earth and Planetary Science Letters* 235: 700-714.

Ingerson, R., F.J. Pearson. 1964. Estimation of age and rate of motion of groundwater by the ^{14}C method. In: Y.Miyake, T. Koyama (eds), Recent Research in the Field of Hydroshpere, Atmosphere, and Nuclear Geochemistry, Marusen, Tokyo, 404 pages.

James, E.R., M. Manga, T.P. Rose. 1999. CO_2 degassing in the Oregon Cascades. *Geology* 27(9): 823-826.

Javoy, M., F. Pineau, I. Iiyama. 1978. Experimental determination of the isotopic fractionation between gaseous CO_2 and carbon dissolved in tholeiitic magma. *Contributions to Mineralogy and Petrology* 67: 35-39.

Javoy, M., F. Pineau, H. Delorme. 1986. Carbon and nitrogen isotopes in the mantle. *Chemical Geology* 57: 41-62.

Kalin, R.M. 2000. Radiocarbon dating of groundwater systems. Chapter 4, in: P.G. Cook, A.L. Herczeg (eds), Environmental Tracers in Subsurface Hydrology, Kluwer Academic Publishers, Boston, 529 pages.

Karlen, I., I.U. Olsson, P. Kallburg, S. Kilici. 1968. Absolute determination of the activity of two ^{14}C dating standards. *Arkiv Geofysik* 4: 465-471.

Keeling, C.D. 1958. The concentration and isotopic abundance of atmospheric carbon dioxide in rural areas. *Geochimica et Cosmochimica Acta* 13: 322-334.

Kendall, C., E.A. Caldwell. 1998. Fundamentals of isotope geochemistry. Chapter 2 in: C. Kendall, J.J. McDonnell (eds.), Isotope Tracers in Catchment Hydrology, Elsevier Science B.V., Amsterdam, 839 pages.

Kennedy, C. 2004. Pilot project on groundwater dating in confined aquifers of the North Carolina coastal plain. MSc thesis, North Carolina State University, 211 pages.

Keywood, M.D., L.K. Fifield, A.R. Chivas, R.G. Cresswell. 1998. Fallout of Chlorine 36 to the Earth's surface in the southern hemisphere. *Journal of Geophysical Research* 103(D7): 8281-8286.

Knies, D.L., D. Elmore, P. Sharma, S. Vogt, R. Li, M.E. Lipshutz, G. Petty, J. Farrell, M.C. Monaghan, S. Fritz, E. Agee. 1994. ^{7}Be, ^{10}Be, and ^{36}Cl in precipitation. *Nuclear Instruments and Methods in Physics Research* 92: 340-344.

Kunkler, J.L. 1969. The sources of carbon dioxide in the zone of aeration of the Bandelier Tuff, near Los Alamos, New Mexico. U.S. Geological Survey professional papers 650-B: B185-B188.

Lachniet, M.S., W.P. Patterson. 2002. Stable isotope values of Costa Rican Surface Waters. *Journal of Hydrology* 260: 135-150.

Libby, W.F., E.C. Anderson, J.R. Arnold. 1949. Age determination by radiocarbon concentration: World-wide assay of natural radiocarbon. *Science* 109: 227.

Lin, Y., Y. Guan, L.A. Leshin, Z. Ouyang, D. Wang. 2005. Short-lived chlorine-36 in a Ca- and Al-rich inclusion from the Ningqiang carbonaceous chondrite. *Proceedings from the National Academy of Sciences of the United States of America* 102(5): 1306-1311.

Loescher, H.W., S.F. Oberbauer, H.L. Gholz, B. Clark. 2003. Environemental controls on net ecosystem-level carbon exchange and productivity in a Central American tropical wet forest. *Global Change Biology* 9: 396-412

McIntosh, J.C., L.M. Walter. 2006. Paleowaters in Silurian-Devonian carbonate aquifers: Geochemical evolutions of groundwaters in the Great Lakes region since the late Pleistocene. *Geochimica et Cosmochimica Acta* 70: 2454-2479.

McDade, L.A., G.S. Hartshorn. 1994. La Selva Biological Station. Chapter 2 In: McDade, L.A., Bawa, K.S., Hespenheide, H.A., Hartshorn, G.S. (eds), La Selva: Ecology and Natural History of a Neotropical Rainforest, The University of Chicago Press, Chicago, 486 pages.

McNichol, A.P., G.A Jones. 2003. Measuring ^{14}C in seawater by Accelerator Mass Spectrometry. WOCE Hydrographic Operations and Methods manual, WOCE Hydrographic Programme Office, WOCE Report No. 68/91, Woods Hole Oceanographic Institution, Woods Hole, MA.

Olsson, I.U. 1970. The use of Oxalic acid as a Standard. In: Olsson, I.U. (eds), Radiocarbon Variation and Absolute Chronology, Nobel Symposium, 12th Proceeding, John Wiley and Sons, New York, page 17.

Ohsawa, S., K. Kazahaya, M. Yasuhara, T. Kono, K. Kitaoka, Y. Yusa, K. Yamaguchi. Escape of volcanic gas into shallow groundwater systems at Unzen Volcano (Japan): Evidence from chemical and stable isotope compositions of dissolved inorganic carbon. 2002. *Limnology* 3: 169-173.

Parker, J.M., S.S. Foster, A. Gomez-Cruz. 1988. Key hydrological features of a recent andesitic complex in Central America. *Geolis* 2(1): 13-23.

Parkhurst, D.L., L.N. Plummer. 1983. Geochemical models. Chapter 9 in: W.M. Alley (eds.), Regional Groundwater Quality, Van Nostrand Reinhold, New York, 634 pages.

Pearson, F.J., D.E. White. 1967. Carbon-14 ages and flow rates in Carrizo Sand, Atascosa County, Texas. *Water Resources Research*. 3(1): 251-261.

Phillips, F.M., F. Goff, F. Vuataz, H.W. Bentley, D. Elmore, H.E. Grove. 1984. ^{36}Cl as a tracer in geothermal systems: Example from Valles Caldera, New Mexico. *Geophysical Research Letters* 11(12): 1227-1230.

Phillips, F.M., H.W. Bentley, S. N. Davis, D. Elmore, G.B. Swanick. 1986. Chlorine 36 dating of very old groundwater 2. Milk River Aquifer, Alberta Canada. *Water Resources Research* 22(13): 2003-2016.

Phillips, F.M. 2000. Chlorine-36. Chapter 10 in: P.G. Cook, A.L. Herczeg (eds), Environmental Tracers in Subsurface Hydrology, Kluwer Academic Publishers, Boston, 529 pages.

Pineau, F. M. Javoy. 1983. Carbon isotopes in mid ocean ridge basalts. *Earth and Planetary Science Letters* 62: 239-257.

Pineau, F., M. Javoy. 1986. The volatile record of a "popping" rock from the mid-Atlantic ridge at 15ºN: concentrations and isotopic composition. *Terra Cognita* 6: 191.

Plummer, L.N., J.F. Busby, R.W. Lee, B.B. Hanshaw. 1990. Geochemical modeling of the Madison aquifer in parts of Montana, Wyoming, and South Dakota. *Water Resources Research* 26(9): 1981-2014.

Plummer, L.N., E.C. Prestemon, D.L. Parkhurst. 1994. An Interactive Code (NETPATH) for Modeling Net Geochemical Reactions Along a Flowpath, Version 2.0. U.S. Geological Survey Water Resources Investigations Report 94-4169, 130 pages.

Plummer, L.N., C.L. Sprinkle. 2001. Radiocarbon dating of dissolved inorganic carbon in groundwater from confined parts of the Upper Floridian aquifer, Florida, USA. *Hydrogeology Journal* 9: 127-150.

Poorter, R.P.E., J.C. Varekamp, R.J. Poreda, M.J. Van Bergen, R. Kreulen. 1991. Chemical and isotopic compositions of volcanic gases from the east Sunda and Banda arcs, Indonesia. *Geochimica et Cosmochimica Acta* 55: 3785-3807.

Pringle, C.M., P. Paaby-Hansen, P.D. Vaux, C.R. Goldman. 1986. In situ nutrient assays of periphyton growth in a lowland Costa Rican stream. *Hydrobiologia* 134: 207-213.

Pringle, C.M., F. J. Triska, G. Browder. 1990. Spatial variation in basic chemistry of streams draining a volcanic landscape on Costa Rica's Caribbean slope. *Hydrobiologia* 206: 73-85

Pringle, C.M., F.J. Triska. 1991. Effects of geothermal groundwater on nutrient dynamics of a lowland Costa Rican stream. *Ecology* 72: 951-965.

Pringle, C.M., G.L. Rowe, F.J. Triska, J.F. Fernandez, J. West. 1993. Landscape linkages between geothermal activity and solute composition and ecological response in surface waters draining the Atlantic slope of Costa Rica. *Limnology and Oceanography* 38(4): 753-774.

Purdy, C.B., G.R. Helz, A.C. Mignerey, P.W. Kubik, D. Elmore, P. Sharma, T. Hemmick. 1996. Aquia aquifer dissolved Cl^- and $^{36}Cl/Cl$: Implications for flow velocities. *Water Resources Research* 32(5): 1163-1171.

Rao, U., U. Fehn, R.T.D. Teng, F. Goff. 1996. Sources of chloride in hydrothermal fluids from the Valles caldera, New Mexico: a ^{36}Cl study. *Journal of Volcanology and Geothermal Research* 72: 59-70.

Rose, T.P., M.L. Davisson. 1996. Radiocarbon in hydrologic systems containing dissolved magmatic carbon dioxide. *Science* 273: 1367-1370.

Rymer, H., J. Cassidy, C.A. Locke, M.V. Barboza, J. Barquero, J. Brenes, R. Van der Laat. 2000. Geophysical studies of the recent 15-year eruptive cycle at Poas Volcano, Costa Rica. *Journal of Volcanology and Geothermal Research* 97: 425-442.

Sanford, R.L. Jr., P. Paaby, J.C. Luvall, E. Phillips. 1994. Climate, geomorphology, and aquatic systems. Chapter 3 in: McDade, L.A., Bawa, K.S., Hespenheide, H.A., Hartshorn, G.S. (eds), La Selva: Ecology and Natural History of a Neotropical Rainforest, The University of Chicago Press, Chicago, 486 pages.

Santos, F.J., J.M. Lopez-Guitierrez, M. Garcia-Leon, Ch. Schnabel, H.-A. Synal, M. Suter. 2004. Analysis of ^{36}Cl in atmospheric samples from Seville (Spain) by AMS. *Nuclear Instruments and Methods in Physics Research* 223-224: 501-506.

Schwendenmann, L., E. Veldkamp. 2006. Long-term CO_2 production from deeply weathered soils of a tropical rain forest: evidence for a potential positive feedback to climate warming. *Global Change Biology* 12: 1878-1893.

Skoog, D.A., D.M. West. 1980. Selected methods of analysis, in: Analytical Chemistry, Saunders College, Philidelphia, pages 571-620.

Sollins, P., R. Radulovich. 1988. Effects of soil physical structure on solute transport in a weathered tropical soil. Soil *Science Society of America Journal* 52: 1168-1173

Sollins, P., M.F. Sancho, Ch.R. Mata, R.L. Sanford Jr. 1994. Soils and soil process research. Chapter 4 in: McDade, L.A., Bawa, K.S., Hespenheide, H.A., Hartshorn, G.S. (eds), La Selva: Ecology and Natural History of a Neotropical Rainforest, The University of Chicago Press, Chicago, 486 pages.

Spotl, C. 2005. A robust and fast method of sampling and analysis of $\delta^{13}C$ of dissolved inorganic carbon in ground waters. *Isotopes in Environmental and Health Studies* 41(3): 217-221.

Standard Methods for the Examination of Water and Wastewater, 20th Edition, Method 4110 B –Determination of anions by ion chromatography, Ion chromatography with chemical suppression of eluent conductivity,1998.

Standard Methods for the Examination of Water and Wastewater, 20th Edition, Method 5310B – Total Organic Carbon (TOC), High-Temperature Combustion Method, 1998.

Sumino, H., K. Notsu, S. Nakai, M. Sato, K. Nagao, M. Hosoe, H. Wakita. 2004. Noble gas and carbon isotopes of fumarolic gas from Iwojima volcano, Izu-Ogasawara arc, Japan: implication for the origin of unusual arc magmatism. *Chemical Geology* 209: 153-174.

Suter, M., J. Beer, G. Bonani, H.J. Hofmann, D. Michel, H. Oeschger, H.A. Synal, W. Wolfli. 1987. ^{36}Cl studies at ETH/SIN-AMS facility. *Nuclear Instruments and Methods in Physics Research* B29: 211-215.

Tamers, M.A. 1975. Validity of radiocarbon dates on groundwater: *Geophysical Surveys* 2: 217-239.

Tan, F.C. 1989. Stable carbon isotopes in dissolved inorganic carbon in marine and estuarine environments. Chapter 5 in: P. Fritz, J.Ch. Fontes (eds), Handbook of Environmental Isotope Geochemistry, Elsevier, New York, 428 pages.

Torgersen, T., M.A. Habermehl., F.M. Phillips, D. Elmore, P. Kubik, B.G. Jones, T. Hemmick, H.E. Grove. 1991. Chlorine 36 dating of very old groundwater 3. Further studies in the Great Artesian Basin, Australia. *Water Resources Research* 27(12): 3201-3213.

Veneklaas, E.J. 1990. Nutrient fluxes in bulk precipitation and throughfall in two montane tropical rain forests, Columbia. *Journal of Ecology* 78: 974-992.

Wassenaar, L., R. Aravena, P. Fritz, J. Barker. 1990. Isotopic composition (^{13}C, ^{14}C, ^{2}H) and geochemistry of aquatic humic substances from groundwater. *Organic Geochemistry* 15(4): 383-396.

Williams-Jones, G., J. Stix, M. Heiligmann, A. Charland, B.S. Lollar, N. Arner, G. Garzon, J. Barquero, E. Fernendez. 2000. A model of diffuse degassing at three subduction-related volcanoes. *Bulletin of Volcanology* 62: 130-142.

Weyl, R. 1980. Southern Central America. Chapter 4 in: Geology of Central America, Gebruder Borntraeger, Berlin-Nikolassee, 371 pages.

Appendices

Appendix 1.

Water chemistry results

Table A1.1. All samples collected March 2006 except BCNP 1 which was collected December 2006.

- Well 20 DIC(calc) was calculated using the pH from the Salto seep (no field measurement of pH at Well 20).
- Anion/cation and TOC data are from results sent from the Analytical Services Lab (NCSU-SS) that were received 5/23/06.
- 36Cl data is reported here as NR/S which is equal to the 36Cl/Cl ratio multiplied by a factor of 10^{15}. (http://www.physics.purdue.edu/primelab/results/weburs_help.html)
- TOC, NH4, NO3, and tS were averaged from the analytical results of two samples from each site. For TOC and NO3, there were 3 cases in which one sample had a concentration below the detection limit and the other did not (well 18 and Arbo weir for TOC, Salto seep for NO3). In these cases, the average concentration given here is the average of half the detection limit (0.5 for TOC and 0.05 for NO3) and the measured concentration that was above this limit for one of the two replicates.
- Reported CFC and SF6 concentrations are mean values from sample replicates (vary from 1 to 3 replicates per location). The individual results, calculated mean, standard deviation, and coefficient of variance are shown on sheet "CFC and SF6 variance."
- $\delta^{18}O$ data was averaged from the results of two samples that were taken from each site.

	Diss. gases	Diss. O_2		Spec. Cond.	Temp	Alk	pH	DIC mM
Sampling location	mm of Hg	mg/L	mM	µS	˚C	mN		(calc)
Well 11	733	0.50	0.02	350.2	25.4	2.62	5.98	8.77
Well 13	734	0.57	0.02	160.8	24.9	1.44	5.93	5.22
Well 14	757	2.07	0.06	15.0	24.9	0.038	4.85	1.70
Arbo weir					26.3	2.41	6.43	4.42
Well 16	764	2.23	0.07	1.0	25.0	<0.002	4.61	<1.49
Well 7	764	2.84	0.09	12.3	24.7	<0.002	4.45	<3.01
Well 18	748	1.01	0.03	35.3	24.8	0.104	5.18	1.74
Taco weir	741	8.99	0.28	7.8	24.7	0.04	5.63	0.26
Well 20	757	2.87	0.09	455.0	25.3	3.78	6.05	11.32
Salto Seep	769	4.76	0.15	484.1	25.7	3.9	6.05	11.68
Well 30	775	3.53	0.11	62.2	24.8	0.31	5.78	1.47
Saltito seep	732	5.42	0.17	180.6	25.1	1.47	6.50	2.50
Guacimo spring	781	4.09	0.13	624.1	25.8	5.23	6.13	13.92
BCNP 1	723	3.34	0.10	9.9	22.4	0.02	4.70	1.82

Table A1.1 continued.

Sampling location	Cl		SO4		Ca		K	
	mg/L	mM	mg/L	mM	mg/L	mM	mg/L	mM
Well 11	16.4	0.4626	8.1	0.0843	24	0.5988	3.5	0.0895
Well 13	7.2	0.2031	2.2	0.0229	13.6	0.3393	0.81	0.0207
Well 14	2.3	0.0649	1.1	0.0115	1	0.0250	<0.1	<0.0026
Arbo weir	15.2	0.4287	3.9	0.0406	18.7	0.4666	4.5	0.1151
Well 16	1.8	0.0508	1.2	0.0125	1	0.0250	<0.1	<0.0026
Well 7	2.1	0.0592	0.5	0.0052	0.44	0.0110	<0.1	<0.0026
Well 18	2.1	0.0592	5.6	0.0583	2.1	0.0524	<0.1	<0.0026
Taco weir	2.2	0.0621	0.4	0.0042	0.63	0.0157	0.3	0.0077
Well 20	23.6	0.6657	8.4	0.0874	21.8	0.5439	5.9	0.1509
Salto Seep	25.8	0.7277	7.7	0.0802	25.9	0.6462	7.2	0.1842
Well 30	3	0.0846	6.8	0.0708	4	0.0998	0.66	0.0169
Saltito seep	10.6	0.2990	2.4	0.0250	10.2	0.2545	2.4	0.0614
Guacimo spring	32.4	0.9139	13.8	0.1437	31.3	0.7810	9.4	0.2404
BCNP 1	1.95	0.0550	0.4	0.0042	0.17	0.0042	0.62	0.0159

Table A1.1 continued.

Sampling location	Mg		Na		Total organic Carbon (TOC)		NH4	
	mg/L	mM	mg/L	mM	mg C/L	mmoles C/L	mg N/L	mmole N/L
Well 11	16	0.6583	23.4	1.0178	<1.0	<0.0833	<0.1	<0.0071
Well 13	9	0.3703	9.2	0.4002	1.6	0.1332	<0.1	<0.0071
Well 14	0.25	0.0103	2.6	0.1131	2.4	0.1998	<0.1	<0.0071
Arbo weir	16.1	0.6624	21.4	0.9308	0.9	0.0749	<0.1	<0.0071
Well 16	0.27	0.0111	0.96	0.0418	<1.0	<0.0833	<0.1	<0.0071
Well 7	0.27	0.0111	1.4	0.0609	2.4	0.1998	<0.1	<0.0071
Well 18	0.14	0.0058	5.9	0.2566	1.0	0.0833	<0.1	<0.0071
Taco weir	0.37	0.0152	1.6	0.0696	4.7	0.3913	<0.1	<0.0071
Well 20	25.7	1.0574	37.8	1.6442	<1.0	<0.0833	<0.1	<0.0071
Salto Seep	28.5	1.1726	33.6	1.4615	<1.0	<0.0833	<0.1	<0.0071
Well 30	2.1	0.0864	4.9	0.2131	3.8	0.3164	<0.1	<0.0071
Saltito seep	9.4	0.3868	13.2	0.5742	5.1	0.4246	<0.1	<0.0071
Guacimo spring	38.9	1.6005	44.8	1.9487	<1.0	<0.0833	<0.1	<0.0071
BCNP 1	0.245	0.0101	0.87	0.0378	0.5	0.0441		

Table A1.1 continued.

Sampling location	NO3		Total Sulfur (tS)		DIC from WHOI	
	mg N/L	mmoles N/L	mg S/L	mmoles S/L	mM	mM (no HgCl2)
Well 11	<0.10	<0.0071	2.70	0.0842	6.48	6.32
Well 13	<0.10	<0.0071	0.90	0.0281	4.07	
Well 14	0.11	0.0079	0.35	0.0109	1.90	
Arbo weir	0.12	0.0086	1.80	0.0561	3.91	
Well 16	0.14	0.0100	0.38	0.0119	1.52	1.54
Well 7	0.37	0.0264	0.14	0.0044	1.62	
Well 18	<0.10	<0.0071	3.20	0.0998	1.80	
Taco weir	<0.10	<0.0071	0.27	0.0084	0.24	
Well 20	<0.10	<0.0071	3.10	0.0967	8.63	
Salto Seep	0.09	0.0064	3.40	0.1060	9.24	
Well 30	<0.10	<0.0071	2.20	0.0686	1.71	
Saltito seep	<0.10	<0.0071	1.10	0.0343	2.26	
Guacimo spring	0.11	0.0079	5.00	0.1559	10.70	10.66
BCNP 1						

Table A1.1 continued.

Sampling location	del ^{13}C		^{14}C			
	‰ (VPDB)	‰ (no HgCl2)	F Modern	F mod (no HgCl2)	Age	Age (no HgCl2)
Well 11	-7.58	-7.63	0.217 ± 0.001	0.218043	12300	12250
Well 13	-15.49		0.599 ± 0.002		4110	
Well 14	-25.54		1.116 ± 0.004		>Mod.	
Arbo weir	-4.39		0.177 ± 0.004		13900	
Well 16	-24.34	-24.44	1.169 ± 0.004	1.16692	>Mod.	>Mod.
Well 7	-26.00		1.171 ± 0.003		>Mod.	
Well 18	-23.45		0.997 ± 0.003		30	
Taco weir	-22.35		1.087 ± 0.003		>Mod.	
Well 20	-6.80		0.180 ± 0.001		13750	
Salto Seep	-5.24		0.104 ± 0.001		18150	
Well 30	-20.20		0.834 ± 0.003		1460	
Saltito seep	-5.83		0.297 ± 0.002		9760	
Guacimo spring	-4.89	-4.89	0.0798 ± 0.001	0.079601	20300	20300
BCNP 1			1.136 ± 0.003			

Table A1.1 continued.

Sampling location	^{36}Cl	^{18}O	Average CFC-12	Average CFC-11	Average CFC-113	Average SF6 (NOAA scale)	Tritium	
	NR/S	‰(VSMOW)	pmol/kg	pmol/kg	pmol/kg	pmol/L	TU	+/-
Well 11	24	-4.99	0.137611	0.446240	0.017194	0.1692	1.05	0.10
Well 13	27	-4.53	1.032214	1.364627	0.157924	0.9238	0.91	0.10
Well 14	10	-4.35	1.712322	3.211141	0.247198	1.4788	0.76	0.10
Arbo weir	26	-4.33	1.022875	1.761875	0.138699		0.69	0.10
Well 16	112	-4.24	1.621089	3.017366	0.243003	0.9309	0.72	0.10
Well 7	228	-4.35	1.664490	3.017713	0.257219	1.0980	0.99	0.10
Well 18	7	-4.37	1.689792	2.938706	0.244122	1.5183	1.10	0.10
Taco weir	160	-3.07	1.560402	3.098139	0.239465		0.99	0.10
Well 20	17	-4.63	0.829012	1.243843	0.101139	0.6083	0.61	0.10
Salto Seep	13	-4.79	0.166266	0.516557	0.016076	0.0329	0.51	0.10
Well 30	590	-4.17	1.448459	3.129467	0.187322	1.1830	0.66	0.10
Saltito seep	69	-4.27	1.172018	1.865063	0.154837	0.9595	0.81	0.10
Guacimo spring	17	-4.26	0.078149	0.489064	0.011883	0.0104	0.36	0.10
BCNP 1	130							

Appendix 2

Trial precipitation of silver-chloride

The ^{36}Cl analysis required that chloride be precipitated out of water samples taken from the study area in the form of silver chloride (AgCl). A minimum of 2-5mg of AgCl is required for ^{36}Cl analysis by Prime Lab at Purdue University (http://www.physics.purdue.edu/primelab/introduction/prices.html). The locations from which samples were taken have previously been found to have chloride concentrations ranging from 0.05-0.90 mM. Fully precipitating all the chloride in one liter of water with these concentrations would yield 7 to 129 mg of AgCl, but whether all of this precipitate could be recovered was not known. Therefore, four laboratory experiments were conducted in which AgCl was precipitated from test solutions of known chloride (NaCl) concentration. The precipitate was then collected, dried, and weighed to determine the percent recovery of the AgCl precipitated from each of the test solutions. The results were used to plan what volume of water should be collected at La Selva to ensure sufficient AgCl for ^{36}Cl analysis.

AgCl was precipitated from test solutions with known chloride concentrations representative of some of those to be sampled at La Selva, 0.05 mM (well 7), 0.07 mM (well 8), 0.40 mM (well 1), and 0.9 mM (Guacimo Spring). The chloride from these waters was precipitated as AgCl. Before the precipitation was carried out, 0.5 N nitric acid was added to the solution to reduce the pH to around 3 to prevent interference from anions of weak acids, such as CO_3^{2-} (Skoog and West 1980). After the precipitation was completed the AgCl was recovered and transferred to previously weighed bottles of the

same type that were used to store and transport the AgCl samples from the study area. The AgCl was then dried and weighed to determine how much was recovered. Four experiments were done (Experiments 1, 2, 3, and 4), each with 3-5 test solutions of known chloride concentration. This appendix gives the procedures used and results obtained for the four experiments.

Preparation of 0.5N HNO_3 from HNO_3(optima):

Materials

- 125ml Nalgene bottle with dropping pipette (dropper) in the cap (Fisher Scientific cat. no. 03-337-10C) cleaned with soap and rinsed thoroughly with deionized water prior to use.
- 1 disposable plastic pipette marked at 1.77ml (marked off in 0.5ml increments from the factory).
- 250ml beaker cleaned with soap and rinsed thoroughly with deionized water prior to use.
- HNO_3(optima), ≈15.8N or 68-70% HNO_3, ≤0.08ppm chloride, Fisher Scientific cat. no. A200-500
- Latex gloves
- 100ml of deionized water
- ≈125ml tap water
- Digital Balance

Procedure

1. Prepare 100ml of deionized water in the 125ml Nalgene dropper bottle, a disposable pipette marked at 1.77ml, and the beaker with about 125ml of tap water for disposal of the excess HNO_3.
2. Place the materials described above on a paper towel in an exhaust hood along with the closed bottle of HNO_3(optima). Make sure the exhaust fan is on and the dropper bottle is uncapped.
3. Wearing latex gloves, remove the cap and seal from the HNO_3(optima) bottle, pour about 5-10ml of the solution from the HNO_3(optima) bottle into its bottle cap.
4. Rinse the pipette with HNO_3(optima) once, then draw 1.5 ml of HNO_3(optima) from the bottle cap and empty the pipette into the dropper bottle, then draw 1.77ml of HNO_3(optima) from the bottle cap with the pipette and empty it into the dropper bottle for a total of 3.27ml of HNO_3(optima) solution added to the 100ml of deionized water.
5. Pour the excess HNO_3(optima) remaining in the bottle cap into the beaker filled with tap water, place the seal and then the cap on the HNO_3(optima) bottle and tighten the cap securely.
6. Close the dropper bottle, tighten the cap securely.
7. Dispose of the pipette and wipe down the outside of the closed dropper bottle and HNO_3(optima) bottle as well as any other surfaces used.

8. Pour the water used to dispose of the excess HNO_3(optima) down the drain then clean and rinse the beaker.

The resulting solution was 103.27ml of 0.50N HNO_3.

In experiment 1, the volume of deionized water in step one was measured volumetrically. In experiments 2 and 3, the volume of deionized water in step 1 was measured gravimetrically to get a more precise concentration, and 3.25ml of HNO_3(optima) was added instead of 3.27ml. The solution of HNO_3 prepared for Experiment 3 was also used in Experiment 4.

Table A2.1. Mixing 0.5N HNO_3

Experiment number	Density of water (g/ml) at 23˚ C	Mass of deionized water (g)	Volume of deionized water (ml)	HNO3 (optima) concentration (N)	Desired HNO3 concentration (N)	Necessary HNO3 (optima) addition to deionized water for desired concentration (ml)	HNO3 (optima) added (ml)	Resultant volume (ml)	Resultant concentration (N)
1	0.997538	NA	100	15.8	0.5	3.268	3.27	103.25	0.50
2	0.997538	99.740	99.986	15.8	0.50	3.268	3.25	103.24	0.50
3	0.997538	99.757	100.003	15.8	0.50	3.268	3.25	103.25	0.50

Preparation of test solutions of known chloride concentration from 0.0282M Cl standard:

Materials

- Four 1000ml polystyrene jars with watertight lids (Fisher Scientific cat. no. 02-912-266), cleaned with soap and rinsed thoroughly with deionized water then

rinsed again with dilute HNO_3 (about 300ml deionized water and 3ml 0.5N HNO_3 swirled around in jar, being sure to rinse all surfaces for about 5 minutes).

- Aqueous Cl standard (SPEX CertiPrep cat. no. AS-CL9-2X), 28.2mM (1mg/ml), made from NaCl.
- 1 disposable plastic pipette
- Labeling tape and pen
- 1000ml graduated cylinder
- Digital balance

Procedure

1. Prepare four clean 1L polystyrene jars with deionized water measured volumetrically with a 500 or 1000ml graduated cylinder, a disposable pipette marked at 1.75ml, and the bottle of aqueous chloride standard solution.
2. From each of the polystyrene jars, using the pipette, draw and dispose of an amount of water equal to the amount of chloride standard that will be added to that jar. For example, 1.75 ml of water was drawn from the jar that held Solution 1.1 (Table 2).
3. Once the appropriate amount of water has been drawn from each of the jars rinse the pipette with the chloride standard once and then use it to add the appropriate volume of chloride standard for each of the test solutions (Table 2). The new volume of the test solution should be equal to the initial volume of deionized water from step one.

4. Record the solution number, Cl concentration, and volume of each solution; label the lid of each jar with this information also.
5. Tightly close the jars holding the solutions and shake.
6. Dispose of the pipette used and tightly close the bottle containing the chloride standard.

The solutions mixed in the jars were the test solutions with known chloride concentrations from which AgCl was precipitated to determine Cl recovery via the precipitation process.

In Experiment 1, water volumes were such that the jars could not be closed without spilling some of the solution. In order to maintain a known volume, some solution was removed with a disposable pipette and discarded in order to close the jars without spilling (Table 2). Solutions 1-4 had Cl concentrations representative of water from the following sampling locations at La Selva

Solution 1 – rain water and/or well 7

Solution 2 – rain water and /or well 7

Solution 3 – well 8

Solution 4- Guacimo Spring

In Experiment 2, the polystyrene jars were substituted with 1 gallon (~4L) plastic jugs (cleaned in the same manner as the polystyrene jars in Experiment 1) for the two low Cl test solutions (0.05mM and 0.07mM) in order to precipitate AgCl from a larger volume

of water (~3500ml) and thereby increase the amount of precipitate produced by the precipitation process. The volume of chloride standard added to each of the test solutions in step 3 was determined gravimetrically using a density of 0.9982g/ml at 22˚C for the chloride standard. That density was measured in the lab using a 10ml graduated cylinder and a digital balance. This was done for Experiments 3 and 4 also. Solutions 1-4 had Cl concentrations representative of water from the following sampling locations at La Selva.

Solution 1 – rainwater and/or well 7

Solution 2 – Well 8

Solution 3 – Well 1

Solution 4 – Guacimo Spring

In Experiment 3, two 1 gallon plastic jugs and two ½ gallon jugs, cleaned in the same manner as the polystyrene jars in Experiment 1, were use for the two low Cl and two high Cl test solutions respectively instead of 1L polystyrene jars. This was done in order to precipitate AgCl from a larger volume of water, thereby increasing the amount of precipitate produced by the precipitation process. The AgCl was also easier to scrape from the surface of 1 and ½ gallon jars than the polystyrene jars. Solutions 1-4 had Cl concentrations representative of water from the same sampling locations described in Experiment 2.

In Experiment 4, five 1.1 gallon Rubbermaid containers, cleaned in the same manner as the polystyrene jars in Experiment 1, with dimensions of about 27cm x 17cm x ___ were used instead of polystyrene jars. This was done to precipitate AgCl from a larger volume

and shorter column of water in order to increase the amount of precipitate produced and decrease the time necessary for the precipitate to settle out of the solution prior to its collection. All the test solutions had a Cl concentration of 0.05mM, which is representative of the Cl concentration found at Well 7 at La Selva.

Table A2.2. Preparation of test solutions of known Cl concentration. Experiment 1 consists of solution numbers 1.1-1.4, Experiment 2 consists of solution numbers 2.1-2.4, Experiment 3 consists of solution numbers 3.1-3.4, Experiment 4 consists of solution numbers 4.1-4.5.

Solution number	Cl standard conc. (mM)	Desired solution conc. (mM)	Initial solution volume (ml)	Cl standard needed (ml)	Cl standard needed (g)	H2O removed from jar (ml)	solution volume remaining in jar (ml)	Cl standard added (g)	Cl standard added (ml)	New solution volume (ml)	Final Cl conc. (mM)	Volume of solution removed to fit lid (ml)	Final solution volume (ml)
1.1	28.2	0.05	988	1.752	N/A	1.75	986.25	N/A	1.75	988	0.0499	65	923
1.2	28.2	0.05	962	1.706	N/A	1.7	960.3	N/A	1.7	962	0.0498	30	932
1.3	28.2	0.071	951	2.394	N/A	2.4	948.6	N/A	2.4	951	0.0712	30	921
1.4	28.2	0.9	955	30.479	N/A	30.5	924.5	N/A	30.5	955	0.9006	30	925
2.1	28.2	0.05	3500	6.206	6.195	6	3494	6.000	6.011	3500	0.0484	0	3500
2.2	28.2	0.07	3500	8.688	8.673	8.5	3491.5	8.481	8.496	3500	0.0685	0	3500
2.3	28.2	0.4	900	12.766	12.743	0	900	12.772	12.795	913	0.3953	0	913
2.4	28.2	0.9	900	28.723	28.673	28.5	871.5	28.550	28.600	900	0.8960	0	900
3.1	28.2	0.05	3500	6.206	6.195	6.25	3493.75	6.195	6.206	3500	0.0500	0	3500
3.2	28.2	0.07	3500	8.688	8.673	8.5	3491.5	8.666	8.681	3500	0.0699	0	3500
3.3	28.2	0.4	1500	21.277	21.239	21.25	1478.75	21.255	21.292	1500	0.4003	0	1500
3.4	28.2	0.9	1500	47.872	47.788	47.75	1452.25	47.791	47.875	1500	0.9000	0	1500
4.1	28.2	0.05	1800	3.191	3.186	0	1800	3.548	3.554	1804	0.0556	0	1804
4.2	28.2	0.05	3500	6.206	6.195	0	3500	6.178	6.189	3506	0.0498	0	3506
4.3	28.2	0.05	3500	6.206	6.195	0	3500	6.171	6.182	3506	0.0497	0	3506
4.4	28.2	0.05	3500	6.206	6.195	0	3500	6.179	6.190	3506	0.0498	0	3506
4.5	28.2	0.05	1800	3.191	3.186	0	1800	3.201	3.207	1803	0.0501	0	1803

Precipitation and collection of AgCl:

Materials

- Previously prepared 0.5N HNO_3 solution in dropper bottle
- Previously prepared test solutions of known Cl concentration
- Clean opaque brown plastic bottles, 60ml (Fisher Scientific cat. no. 03-084A), one for each test solution

- $AgNO_3$, 500ml, 0.282N (1ml:10mg Cl) (Fisher Scientific cat. no. LC22725-1)
- pH test strips (0-14pH)
- Plastic policeman
- Rubber policeman
- V-shaped plastic spatula
- Latex gloves
- Digital balance

Procedure

1. Wearing latex gloves open the four jars containing the test solutions by slowly unscrewing the lids (being careful not to spill). Prepare the dropper bottle so that the appropriate volume of 0.5N HNO_3 can be withdrawn and added to the test solutions.
2. Use the pH test strips to measure and record the initial pH of each solution.
3. Add the appropriate volume of 0.5N HNO_3 to each solution then close the jar and mix the solution to lower the pH to about 3.
4. Using the pH test strips, measure and record the pH of each solution to ensure the pH is around 3 (Table 3). If it is not down to 3, add more HNO_3 and measure the pH until it is.
5. Using a pipette, add excess $AgNO_3$ to each solution ($[Ag^+]$ is greater than $[Cl^-]$) (Table 3).

6. Close the jars and tighten them securely. Shake and, in a dark location, allow the precipitate five days to settle, forming a film on the bottom and sides of the container.
7. Label the 60ml brown plastic bottles with the corresponding solution from which the precipitate that each contains was derived. Weigh the empty labeled bottles and record their mass. Handle the bottles and all other materials with latex gloves to minimize error in weighing and sample contamination.
8. After pouring off the overlying water, use the plastic policeman to scrape the film of AgCl precipitate to the outer edge/corner of the jar. This film should still be wet. The precipitate will be in a pile contained in a drop and/or droplets of water.
9. Use the policeman to nudge the droplets of water that contain the precipitate into the spatula.
10. Empty precipitate from the spatula into its corresponding brown plastic bottle. It may be useful to add small amounts of deionized water to recover more precipitate after initial droplets are transferred.
11. Dry the samples by placing the bottles in an oven for five hours at around 70˚C. Remove the bottles and allow them time to cool thoroughly (a few hours). Be sure to maintain the temperature of the oven well below 100ºC so there is no splatter associated with boiling during evaporation.
12. Measure and record the final mass of the bottle and subtract that from the initial mass to get AgCl recovered.

In Experiment 2, steps 8 and 9 were altered as well as the amount of time the precipitate was allowed to settle.

8. Solution 2.1 and 2.2- Allow the AgCl precipitate from Solution 2.1 to settle for four days, and the precipitate from Solution 2.2 to settle for one day. Pour out the water remaining in the jar. Use the rubber policeman to scrape all the precipitate from the bottom and sides and consolidate it into a pile contained within a drop of water, on the side of the jar. Then allow the consolidated precipitate at least a day to air dry completely.

   Solutions 2.3 and 2.4- Allow the AgCl precipitate to settle for two days. At that point pour out the remaining water and allow the jar, and the film of precipitate remaining, at least a day to air dry completely. Use the plastic policeman to scrape the precipitate from the bottom and sides and consolidate it into a pile on the side of the jar.
9. Collect the precipitate by laying the spatula with an edge flat on the side of the jar next to the pile of the precipitate and dumping it into the spatula by slowly rotating the jar.

In Experiment 3, steps 8-12 were altered, as well as the amount of time the precipitate was allowed to settle.

8. After the precipitate has been allowed to settle for three days, pour off the water and allow the jar, and the film of precipitate remaining, to air dry completely.

9. With the jar on its side, use the rubber policeman to scrape all the precipitate off the bottom of the jar and consolidate it into a pile that can be managed with the spatula.
10. Collect the precipitate with the spatula by laying it with an edge flat on the side of the jar next to the precipitate and dumping the precipitate into the spatula by slowly rotating the jar as described in step 9 for the second experiment.
11. Empty the spatula into the bottle associated with the solution from which the precipitate was derived.
12. Measure and record the final mass and subtract that from the initial mass to get the AgCl recovered.

Steps 9-10 were repeated several times in order to collect as much of the precipitate as possible because the effect of static electricity limited the amount of precipitate that could be consolidated into one location.

In Experiment 4 the procedure for precipitation and collection of AgCl was altered beginning with step 8, precipitate was collected in a slightly different manner for Solution 4.1 than for Solutions 4.2-4.5

<u>Solution 4.1</u>

8. After the precipitate has been allowed to settle out of solution for 2 days, pour out the water and allow a few minutes for the surface of the container to dry somewhat.

9. Use the rubber policeman to scrape the precipitate from the bottom and sides of the container into a pile that can be managed with the spatula.
10. Use the spatula to collect the precipitate in a manner similar to that described in step 9 for the second experiment. The rubber policeman may be needed to push the precipitate into the spatula.
11. Empty the spatula into the bottle associated with the solution from which the precipitate was derived.
12. See step 11 from the Experiment 1
13. See step 12 from Experiment 1

Solution 4.2-4.5

8. After the precipitate has been allowed to settle out of solution for the appropriate amount of time (see Table 3), pour out the water
9. While it's still wet, scrape the precipitate from the sides and bottom of the container and consolidate into a pile contained within a drop of water.
10. Place the container in an oven for about five hours at around 60˚C in order to dry the precipitate.
11. Use the spatula to collect the precipitate in a manner similar to that described in step 9 of the second experiment
12. Empty the spatula into the bottle associated with the solution from which the precipitate was derived.
13. See step 11 from Experiment 1
14. See step 12 from Experiment 1

Table A2.3. Precipitation of AgCl

solution number	Water Volume (ml)	Cl conc. (mM)	Initial pH	HNO3 calculated to be needed for pH3 (ml)	HNO3 added (ml)	Final pH	AgNO3 needed for complete precipitation (ml)	AgNO3 added (ml)	Total AgCl precipitate expected (mg)	Initial mass of bottle (g)	Final mass of bottle (g)	AgCl recovered (mg)	% recovery of AgCl	settling time (days)	container type
1.1	988	0.05	8	1.98	2.0	3	0.175	1	7.08						1L polystyrene
1.2	962	0.05	8	1.93	3.0	3	0.171	1	6.89						1L polystyrene
sum (1.1&1.2	1950	0.05	8	3.91	5.0	3	0.346	2	13.97	9.1922	9.1962	4	29	5	
1.3	951	0.071	8	1.91	4.0	3	0.239	1	9.68	9.122	9.1247	2.7	28	5	1L polystyrene
1.4	955	0.9	8	1.91	4.0	3	3.047	5	123.18	9.1674	9.2209	53.5	43	5	1L polystyrene
2.1	3500	0.05	8	7.01	8	2	0.620	2.5	25.08	8.9680	8.982	14	56	4	3.8L plastic jug
2.2	3500	0.07	8	7.01	8	2	0.869	2.5	35.11	NA	NA	0.001	0.003	1	3.8L plastic jug
2.3	912.75	0.4	8	1.83	2	3	1.294	1.5	52.33	9.0470	9.055	8	15	2	1L polystyrene
2.4	900	0.89	8	1.80	3	2	2.840	3	114.80	8.9600	8.991	31	27	2	1L polystyrene
3.1	3500	0.05	8	7.01	8	2	0.620	1.5	25.08	9.010	9.018	8	32	3	3.8 L plastic jug
3.2	3500	0.07	9	7.01	8	2	0.869	1.5	35.11	9.159	9.169	10	28	3	3.8L plastic jug
3.3	1500	0.4	8	3.01	4	2	2.127	2.5	85.99	8.943	8.985	42	49	3	1.9L plastic jug
3.4	1500	0.9	9	3.01	4	2	4.786	4.5	193.48	9.109	9.218	109	56	3	1.9L plastic jug
4.1	1800	0.05	8	3.61	4.5	1	0.319	2.5	12.90	9.174	9.174	0.001	0.008	2	4.2L plastic tray
4.2	3500	0.05	8	7.01	9	1	0.620	2.5	25.08	9.191	9.202	11	44	2	4.2L plastic tray
4.3	3500	0.05	8	7.01	9	2	0.620	2.5	25.08	9.103	9.120	17	68	3	4.2L plastic tray
4.4	3500	0.05	8	7.01	9	1	0.620	2.5	25.08	9.095	9.102	7	28	4	4.2L plastic tray
4.5	1800	0.05	8	3.61	5	2	0.319	2.5	12.90	9.024	9.031	7	54	2	4.2L plastic tray

* In Experiment 2, the weighing of Solution 2 was done by placing the bottle on the digital balance, zeroing it, and then adding the AgCl precipitate, because of that there is no value for initial mass of the empty bottle
* The precipitates from solutions 1.1 and 1.2 were combined into one bottle and weighed together (not separately).

Results

The results from this set of experiments confirms that enough AgCl precipitate can be produced from water samples of adequate size collected at La Selva Biological Station if the precipitate is given enough time to settle out once the $AgNO_3$ is added, if the precipitate is collected in the correct manner, and if the precipitation is done in a container that the precipitate does not adhere to once dry.

Collecting 4 liters of water from the low Cl sampling sites at La Selva allows some room for error with respect to obtaining enough AgCl while not providing too much inconvenience in retrieving the sample. Scraping the precipitate into a pile right after pouring the water off and then letting it dry (see steps 8-10 for the precipitation and collection of solution 4.2-4.5, page 13) produces larger chunks of dried precipitate that are much easier to handle, rather than very fine flakes (see steps 8-10 for the precipitation and collection of Solutions 3.1-3.4) that can easily be affected by static electricity. During the course of these experiments it was also found that the precipitate was more

difficult to retrieve from the 1L polystyrene jars than the other containers. The precipitate seemed to adhere to the surface of these containers.

The materials and procedure used in the precipitation and collection of Solution 4.2 - 4.5 represent the extent of the development of this method. It's possible that settling time and volume can be decreased somewhat while still collecting enough precipitate. However I would not suggest modifying the procedure for the collection of the precipitate once settled (see steps 8-10 for the precipitation and collection of solution 4.2-4.5, page 13), or the container used to carry-out the precipitation unless one is certain that the precipitate will not adhere to it once dried.